ISTANBUL TECHNICAL UNIVERSITY ★ GRADUATE SCHOOL OF SCIENCE ENGINEERING AND TECHNOLOGY

EFFECT OF PHOSPHORESCENT IRIDIUM DOPANT ON CHARACTERISTICS OF ORGANIC LIGHT EMITTING DIODES

M.Sc. THESIS

Ahu Galen ALTAŞ

Department of Nanoscience and Nanoengineering

Nanoscience and Nanoengineering Programme

DECEMBER 2019

ISTANBUL TECHNICAL UNIVERSITY ★ GRADUATE SCHOOL OF SCIENCE ENGINEERING AND TECHNOLOGY

EFFECT OF PHOSPHORESCENT IRIDIUM DOPANT ON CHARACTERISTICS OF ORGANIC LIGHT EMITTING DIODES

M.Sc. THESIS

Ahu Galen ALTAŞ
(513161013)

Department of Nanoscience and Nanoengineering

Nanoscience and Nanoengineering Programme

Thesis Advisor: Prof. Dr. Nilgün KARATEPE YAVUZ
Thesis Co-Advisor: Assoc.Prof. Dr. Emine TEKİN

DECEMBER 2019

ISTANBUL TEKNİK ÜNİVERSİTESİ ★ FEN BİLİMLERİ ENSTİTÜSÜ

ORGANİK ISIK YAYAN DİYOTLARA FOSFORESAN İRİDYUM KATKILANMASININ AYGIT KARAKTERİSTİĞİNE ETKİSİ

YÜKSEK LİSANS TEZİ

Ahu Galen ALTAŞ
(513161013)

Nanobilim ve Nanomühendislik Anabilim Dalı

Nanobilim ve Nanomühendislik Programı

Tez Danışmanı: Prof. Dr. Nilgün KARATEPE YAVUZ
Eş Danışman: Doç. Dr. Emine TEKİN

ARALIK 2019

Ahu Galen ALTAŞ, a M.Sc. student of ITU Graduate School of Science Engineering and Technology student ID 513161013, successfully defended the thesis entitled "EFFECT OF PHOSPHORESCENT IRIDIUM DOPANT ON CHARACTERISTICS OF ORGANIC LIGHT EMITTING DIODES", which she prepared after fulfilling the requirements specified in the associated legislations, before the jury whose signatures are below.

Thesis Advisor :	**Prof. Dr. Nilgün KARATEPE YAVUZ** İstanbul Technical University	……..
Co-advisor :	**Assoc.Prof. Dr. Emine TEKİN** TUBITAK Marmara Research Center	……..
Jury Members :	**Prof. Dr. Esra ZAYİM ÖZKAN** Istanbul Technical University	……..
	Assoc.Prof. Dr. Mustafa ALTUN Istanbul Technical University	…….
	Assoc.Prof. Dr. Elif ALTÜRK TUBITAK Marmara Research Center	……..

Date of Submission : 11 November 2019
Date of Defense : 12 December 2019

To Orçun,

FOREWORD

First of all, I would like to thank Prof.Dr.Nilgün KARATEPE YAVUZ for her encouragement and support. Her faith in me was always felt and I am grateful for that.

I would like to express my deep sense of gratitude to my co-advisor Assoc.Prof.Dr. Emine TEKİN for her help, continuous support, guidance and understanding, and also for giving me morale during the most difficult moments during my thesis. Most importantly, I am grateful for her for giving me a chance to work in the laboratories of TÜBİTAK.

I would also like to thank Dr. Selin PIRAVADILI MUCUR for helping, providing full support and making my days more beautiful in the office. Moreover, my fellow laboratory friends, Rifat KAÇAR, Tülin ATEŞ TÜRKMEN and Emre ASLAN deserve my special thanks for supporting me.

I would like to thank Assoc.Prof.Dr. Elif ALTÜRK for giving me happiness with her high energy, positivity and cheerfulness.

I would also like to thank our project director Dr. Salih DABAK and Photonic Technologies Group responsible Dr. Arif Sinan ALAGÖZ.

A special thank goes to my parents and grandparents for their concern, confidence and support. Finally, I reserve my most sincere thanks to my fiance, Orçun YÜKSEL, for being next to me, supporting me and loving me.

This work was supported by The Scientific and Technological Research Council of Turkey (TUBITAK) & Public Research Grant Group (KAMAG). Project Number: 113G035

November, 2019

Ahu Galen ALTAŞ
(Chemical Engineer)

TABLE OF CONTENTS

Page

ABBREVIATIONS

µm	**:** Micrometer
^{0}C	**:** Celcius degree
A	**:** Amper
AC	**:** Alternating current
Al	**:** Aluminium
Alq_3	**:** Tris-(8-hydroxyquinoline)aluminum
AMOLED	**:** Active-matrix organic light emitting diode
BNC	**:** Binary nano-composite
cd	**:** Candela
CE	**:** Current efficiency
CIE	**:** International Commission on Illumination
cm	**:** Centimeter
DCB	**:** 1,2-Dichlorobenzene
EIL	**:** Electron injection layer
EL	**:** Electroluminescence
EML	**:** Emission layer
EQE	**:** External quantum efficiency
ETL	**:** Electron transport layer
FOLED	**:** Foldable organic light emitting diode
Hex-Ir(piq)$_3$	**:** Tris[2-(4-*n*-hexylphenyl)quinoline)]iridium(III)
HIL	**:** Hole injection layer
HOMO	**:** Highest occupied molecular orbital
HTL	**:** Hole transport layer
ITO	**:** Indium tin oxide
L	**:** Luminescence
LiF	**:** Lithium fluoride
lm	**:** Lumen
LUMO	**:** Lowest unoccupied molecular orbital
m	**:** Meter
mA	**:** Miliamper

mbar : Milibar

MEH-PPV : Poly[2-methoxy-5-(2-ethylhexyloxy)-1,4-phenylenevinylene]

nm : Nanometer

NPD : N,N′-Di(1-naphthyl)-N,N′-diphenyl-(1,1′-biphenyl)-4,4′-diamine

OLED : Organic light emitting diode

PE : Power efficiency

PEDOT:PSS : Poly(2,3-dihydrothieno-1,4-dioxin)-poly(styrenesulfonate)

PEI : Poly(ethyleneimine)

PLED : Polymer light emitting diode

PMOLED : Passive-matrix organic light emitting diode

RGB : Red-green-blue

rpm : Round per minute

s : Second

SMOLED : Small molecule organic light emitting diode

TFT : Thin film transistor

TNC : Ternary nano-composite

TOLED : Transparent organic light emitting diode

TPBi : 2,2′,2"-(1,3,5-Benzinetriyl)-tris(1-phenyl-1-H-benzimidazole)

TPD : N,N′-Bis(3-methylphenyl)-N,N′-diphenylbenzidine

V : Volt

V_2O_5 : Vanadium pentoxide

W : Watt

WL_p : Peak wavelenght

ZnO : Zinc oxide

SYMBOLS

J	**:** Current density
I	**:** Current
$\mathbf{M_w}$	**:** Molecular weight
$\mathbf{N_e}$	**:** Number of injected electrons
$\mathbf{N_p}$	**:** Number of photons
T	**:** Thickness of organic layer
$\mathbf{V_{on}}$	**:** Turn-on voltage
V	**:** Voltage
$\mathbf{T_g}$	**:** Glass transition temperature
λ	**:** Wavelength
$\boldsymbol{\theta}$	**:** Measurement angle
$\boldsymbol{\hbar}$	**:** Plank constant
c	**:** Speed of light
$\boldsymbol{\eta_{ext}}$	**:** External quantum efficiency
$\mathbf{N_p}$	**:** Number of photons
$\mathbf{N_e}$	**:** Number of electrons
$\mathbf{M_w}$	**:** Molecular weight
$\boldsymbol{\Omega}$	**:** Ohm
$\boldsymbol{\mu}$	**:** Mobility
$\boldsymbol{\varepsilon}$	**:** Relative dielectric constant
$\boldsymbol{\varepsilon_0}$	**:** Permittivity of the free space

LIST OF TABLES

Page

LIST OF FIGURES

Page

EFFECT OF PHOSPHORESCENT IRIDIUM DOPANT ON CHARACTERISTICS OF ORGANIC LIGHT EMITTING DIODES

SUMMARY

Organic light-emitting diodes (OLED) are imaging and lighting technology that was no longer just a subject of research in 1985 when Ching Tang and Steven van Slyke produced efficient thin-film light-emitting diodes. The fact that it can be produced transparent and on a flexible substrate makes the organic light emitting diodes one of the promising displaying technologies for the future. Moreover, organic light emitting diodes have many advantages such as low cost of production due to solution processing methods, high display quality, thinner and lighter weight, faster response time and higher efficieny.

The biggest technical problem that emerges in organic light emitting diodes is the limited life time due to degradation of organic materials. Organic materials used in organic light emitting diodes are sensitive to oxygen and moisture; black spots may form on contact with oxygen and moisture over time and affect the image. In addition, self-degradation of organic materials reduces the life time. However, researchs continue in this regard and the life times of organic light emitting diodes are increasing by time.

Simply, organic light emitting diodes are composed of thin film organic layers between two electrodes with different work functions. Metals with low working function are very sensitive to oxygen and moisture by nature and cause rapid degradation. Inverted organic light emitting diodes have a more stable upper electrode with a high work function, which increases the life time of the device. Also, PEDOT:PSS is unstable hole injection material which used widely for conventional devices. Hence, avoid using PEDOT:PSS in inverted devices increases the life time.

In addition, inverted organic light emitting diodes provide ease of integration in active matrix OLED (AMOLED) displays. AMOLEDs consume less energy compared to other display systems due to the thin film transistor (TFT) in their structures. Therefore, they are more efficient in large display systems.

In AMOLED display systems, colors are controlled by the current given to the three primary color (red, green, blue - RGB) pixels. Due to this current controlled by the thin film transistor, many different colors can be displayed on the screen. For this reason, it is of great importance to fabricate organic light emitting diodes that emits in these three primary colors.

Hex-Ir(piq)$_3$ small molecule was selected for investigation of solution processed red light emitting material for potential applications of AMOLED displays. Limited source about Hex-Ir(piq)$_3$ in the literature was effective in the selection of this

molecule. By using Hex-Ir(piq)$_3$ small molecule, solution based organic light emitting diodes were produced and characterization measurements were performed in conventional and inverted OLED architecture.

In order to understand the characteristic properties of the molecule, first the host-free Hex-Ir(piq)$_3$ solutions were prepared and coated with the spin-coating method with different spin rates. Although the spin rate of 1000 rpm gived the highest eficiency for the fabricated device, there were visible morphological problems in the thin film coating. Since Hex-Ir(piq)$_3$ is a small molecule and generally, the solubility of small molecules is low, it was concluded that the rotation speed of 1000 rpm was not sufficient and the rotation speed of 2500 rpm was determined as the optimum value.

Three different inverted devices were fabricated with host-free Hex-Ir(piq)$_3$ solutions. The first one was fabricated in a simpler structure without the hole transport layer. Considering the low luminescence and efficiency, it was decided to add a hole transport layer and the device was produced by adding TPD as hole transport layer to the structure. Significant improvements in device performance was observed with the addition of the hole transport layer. Finally, the effect of electron injection layer was studied and no significant effect on performance was found.

All fabricated host-free Hex-Ir(piq)$_3$ devices emitted in the red light wavelength range and chromatic coordinates are determined according to the CIE 1931 color standard.

Considering the literature, NPD was used as the first host molecule. Significant luminescence and efficiency values were obtained for this host molecule in conventional architecture. However, in inverted architecture, it was observed that luminescence and efficiency values are reduced significantly even if there is a hole transport layer. In addition, in the electroluminescence characteristic graph, a peak between 400-450 nm was observed with the effect of NPD and the emitted color shifted to pinkish red according to CIE 1931 color coordinates. It was decided that NPD host molecule was not suitable host for this study because of the inverted device performance decrease and peak in the electroluminescence graph.

Finally, the MEH-PPV polymer was tested as a host because of its orange light emission and its high performance in inverted architecture. Firstly, doping ratio in conventional structure was studied. Subsequently, a significant increase in performance was observed by adding TPBi as electron transport layer.

In the inverted devices produced from Hex-Ir(piq)$_3$ doped MEH-PPV solution, the difference of electron injection layer was first tried Then, TPD hole transport layer was added to this device to increase the luminescence.

Compared with host-free Hex-Ir(piq)$_3$, electroluminescence characteristics of MEH-PPV devices doped with Hex-Ir(piq)$_3$ showed that the device produced an orange red radiation. However, a significant shift towards the red zone was observed in the Hex-Ir(piq)$_3$ doped MEH-PPV devices comparing to undoped MEH-PPV, according to the CIE 1931 color coordinates.

In addition to these studies, electron mobility of Hex-Ir(piq)$_3$ doped MEH-PPV thin film was investigated. In accordance with the obtained luminescence and efficiency values, the highest electron mobility was obtained in the device produced with a doping ratio of 20%.

ORGANİK ISIK YAYAN DİYOTLARA FOSFORESAN İRİDYUM KATKILANMASININ AYGIT KARAKTERİSTİĞİNE ETKİSİ

ÖZET

Organik ışık yayan diyotlar (OLED), 1985 yılında Ching Tang ve Steven van Slyke'ın verimli ince film ışık yayan diyot üretmesi ile sadece araştırma konusu olmaktan çıkan görüntüleme ve aydınlatma teknolojisidir. Bükülebilir alt taban üzerine ve şeffaf üretilebilir olması organik ışın yayan diyotları geleceğin görüntüleme teknolojilerinden biri haline getirmektedir. Üstelik organik ışık yayan diyotların, çözeltiden üretim metodlarının kullanımına bağlı olarak üretiminin düşük maliyetli olması, görüntü kalitesinin yüksek olması, daha ince ve hafif olması, tepki süresinin çok daha hızlı olması ve verimli olması gibi bir çok avantajı vardır.

Organik ışık yayan diyotlarda ortaya çıkan en büyük teknik sorun organik materyallerin bozunmasına bağlı olarak yaşam ömrünün limitli olmasıdır. Organik ışık yayan diyotlarda kullanılan organik materyaller oksijen ve neme karşı duyarlı olup, zaman içinde oksijen ve nemle teması halinde siyah noktalar oluşabilmekte ve görüntüyü etkileyebilmektedir. Bunun dışında organik materyallerin kendi bozunmaları da yaşam süresini düşürmektedir. Ancak bu konuda da gelişmeler sürmektedir ve organik ışık yayan diyotların yaşam ömürleri zamanla artmaktadır.

Organik ışık yayan diyotlar en basit ifadeyle farklı iş fonksiyonuna sahip iki elektrot arasında bulunan ince film organik katmanlardan oluşmaktadır. Doğası gereği düşük iş fonksiyonuna sahip metaller oksijen ve neme oldukça duyarlıdır ve hızlı bozunuma sebep olmaktadırlar. Tersinir organik ışık yayan diyotlarlarda yüksek iş fonksiyonuna sahip daha kararlı üst elektrot bulunmaktadır, bu da cihazın yaşam ömrünü arttırmaktadır. Ayrıca, PEDOT:PSS, geleneksel cihazlar için yaygın olarak kullanılan kararsız boşluk enjeksiyon malzemesidir. Dolayısıyla PEDOT:PSS kullanmamak tersinir cihazlarda yaşam ömrünü arttırır.

Ayrıca tersinir yapıdaki organik ışık yayan diyotlar, aktif matris OLED (AMOLED) ekranlarda entegrasyon kolaylığı sağlamaktadır. AMOLEDler yapılarında bulunan ince film transistör (TFT) sayesinde diğer ekran sistemlerine göre daha az enerji harcarlar. Bu sebeple, geniş görüntüleme sistemlerinde daha verimlilerdir.

AMOLED görüntüleme sistemlerinde renkler üç ana renk (kırmızı, yeşil, mavi – RGB) piksele verilen akım ile kontrol edilmektedir. İnce film transistörün kontrol ettiği bu akım sayesinde ekran üzerinde çok farklı renkler görüntülenebilmektedir. Bu sebeple bu üç ana renkte ışıma yapan organik ışık yayan diyotlar üretmek büyük önem arzetmektedir.

Tez çalışması kapsamında, Hex-Ir(piq)$_3$ küçük molekülü, AMOLED ekranların potansiyel uygulamaları için çözelti bazlı kullanılmak üzere kırmızı ışık yayan malzeme olarak seçilmiştir. Bu molekülün seçilmesinde literatürde Hex-Ir(piq)$_3$ hakkında kısıtlı kaynak bulunmasının etkisi olmuştur. Hex-Ir(piq)$_3$ küçük molekülü

kullanılarak geleneksel ve tersinir OLED mimarisinde çözelti bazlı organik ışık yayan diyotlar üretilmiş ve karakterizasyon ölçümleri yapılmıştır.

Molekülün karakteristik özelliklerini anlamak amacı ile ilk olarak katkısız Hex-Ir(piq)$_3$ çözeltisi hazırlanmış ve farklı dönme hızları ile dönel kaplama yöntemi kullanarak kaplanmıştır. Üretilen cihaz için 1000 rpm dönme hızı en yüksek verim değerini verse de kaplanan ince filmde gözle görülür morfolojik sorunlar bulunmaktadır. Hex-Ir(piq)$_3$ bir küçük molekül olduğundan ve genel olarak küçük moleküllerin çözünürlülüğü düşük olduğundan 1000 rpm dönme hızının yeterli gelmediği kanısına varılmış ve 2500 rpm dönme hızı optimum değer olarak belirlenmiştir. Bu mimaride elde edilen parlaklık 55 cd/m^2 olup, akım ve güç verimi ise sırasıyla 0.02 cd/A ve 0.01 lm/W'dır.

Katkısız Hex-Ir(piq)$_3$ çözeltisi ile üç farklı tersinir cihaz üretilmiştir. İlki daha basit yapıda boşluk taşıma katmanı olmaksızın üretilmiştir. Elde edilen parlaklık değeri ve akım verimi sırasıyla, 29.66 cd/m^2 ve 0.04 cd/A'dir. Bu değerlerin düşüklüğü göz önüne alındığında boşluk taşıma katmanı eklenmesine karar verilmiş ve yapıya TPD boşluk taşıma katmanı eklenerek cihaz üretilmiştir. Boşluk taşıma katmanının eklenmesi ile cihaz performansında önemli gelişmeler gözlemlenmiştir. Parlaklık değeri 370.6 cd/m^2'ye ve akım verimi 0.6 cd/A'e yükselmiştir. Son olarak elektron enjeksiyon katmanı değiştirilerek etkisi incelenmiş ve performansta önemli bir etkisi bulunmamıştır.

Üretilen tüm katkısız Hex-Ir(piq)$_3$ cihazları kırmızı ışık dalga boyu aralığında ışıma yapmaktadır ve CIE 1931 renk standardına göre kromatik koordinatları belirlenmiştir.

Literatür dikkate alınarak ilk konak molekül olarak NPD kullanılmıştır. Bu konak molekülü için geleneksel mimaride dikkate değer parlaklık ve verim değerleri elde edilmiştir. Parlaklık değeri ve akım verimi sırasıyla, 1889 cd/m^2'ye 2.78 cd/A'dir. Ancak, tersinir mimaride boşluk taşıma katmanı olsa dahi parlaklık ve verim değerlerinin ciddi şekilde düştüğü gözlemlenmiştir. Ek olarak, elektrolüminesans karakteristik grafiğinde NPD etkisi ile 400-450 nm arasında pik gözlemlenmiş ve CIE 1931 renk koordinatlarına göre ışıma rengi pembemsi kırmızıya doğru kaymıştır. NPD konak molekülünün tersinir yapıdaki performans düşüklüğü ve elektrolüminesans grafiğindeki pik sebebi ile bu çalışma için uygun bir host olmadığına karar verilmiştir.

Son olarak turuncu ışıma yapması ve tersinir mimarideki bilinen yüksek performansı sebebiyle MEH-PPV polimeri konak olarak denenmiştir. İlk olarak geleneksel yapıda doplama oranı çalışılmıştır. %20 doplama oranı ile elektron taşıma katmanı olmaksızın 289 cd/m^2 parlaklık ve 0.09 lm/W güç verimi elde edilmiştir. Daha sonrasında TPBi elektron taşıma katmanı eklenerek performansta dikkate değer bir yükseliş gözlemlenmiştir. Parlaklık değer 1025 cd/m^2'ye ve güç verimi 0.23 lm/W'a yükselmiştir.

Hex-Ir(piq)$_3$ doplanmış MEH-PPV çözeltisinden üretilen tersinir cihazlarda ilk olarak elektron enjeksiyon katmanı farkı denenmiş ve BNC (ikili nano-kompozit) ile üretilen cihazda 672 cd/m^2 parlaklık ve 2.22 cd/A akım verimi elde edilmiştir. Daha sonra bu cihaza TPD boşluk taşıma katmanı eklenerek parlaklığın 1514 cd/m^2'ye yükselmesi sağlanmıştır.

Hex-Ir(piq)$_3$ doplanmış MEH-PPV cihazlarında elektrolüminesans karakteristiği katkısız Hex-Ir(piq)$_3$ cihazı ile karşılaştırıldığında dalga boyunun katkısız olan

cihazda 620 nm olan dalga boyunun 597 nm'ye kaydığı ve cihazın daha turuncumsu kırmızı ışıma yaptığı gözlemlenmiştir. Ancak doplanmamış MEH-PPV ile karşılaştırıldığında elde edilen CIE 1931 renk kordinatlarına göre elde edilen cihazlarda kırmızı bölgeye doğru ciddi bir kayma gözlemlenmiştir.

Bu çalışmalara ek olarak, Hex-Ir(piq)$_3$ katkılanmış MEH-PPV ince filminin elektron hareketliliği incelenmiştir. Elde edilen parlaklık ve verim değerleri ile uyumlu olarak 1.29 x 10^{-6} $cm^2V^{-1}s^{-1}$ değeri ile %20 doplama oranı ile üretilen cihazda en yüksek elektron hareketliliği elde edilmiştir.

.

1. INTRODUCTION

Organic electronics is a growing research topic in the fields of chemistry and physics in the last decades. Until mid-1980's organic electronics appear to be a solely research subject. Researchers thinked there is no practical application for organic semiconductor materials due to their lack of performance and stability compared to conventional inorganic semiconductor materials such as silicone and gallium arsenide. On the other hand, in 1985, Ching Tang and Steven van Slyke demonstrate that efficient thin film light emitting diodes are possible within Eastman Kodak [1]. Even though produced diodes are not sufficient in terms of performance compared to existing technology, it was a promising starting point for commercializing of organic electronics. On behalf of commercializing, primarily researched and funded device in organic electronic is organic light emitting diode (OLED).

Nowadays, OLEDs have become the most promising alternative in next-generation flat-panel displays and solid-state lighting source. OLEDs have major virtues include lightweight, high-speed video rate, high contrast, low power consumption and large viewing angle, compared to traditional electroluminescent (EL) devices [2-4].

1.1 Purpose of the Thesis

Red, green, and blue (RGB) are the primary colors of light. In active-matrix OLED displays, thin film transistor integrated into device and act like a switch which controls current flow from each pixel in order to emit different colors in display. Because of this, it is crucial to fabricate RGB color emitted OLEDs for commercial OLED displays. Due to nature of red fluorescent materials, red dopant usage is limited in the fabrication of red OLED. In addition, solution processable materials are preferable because of low cost application processes and compatibility for flexible OLEDs.

The purpose of this thesis is to investigate the effect of doped red phosphorescent iridium complex on solution processed organic light emitting diodes characteristics.

In this scope, conventional OLEDs, inverted OLEDs and electron only devices were fabricated.

In order to optimize these configurations, the effects of solution concentration, dopant ratio, emitting layer thickness, utilization of electron blocking/hole transport layer, thermal annealing temperature/time and different hosts were investigated systematicaly.

Luminance, power and current efficiencies, external quantum efficiency and electroluminescence characteristics were studied for both conventional and inverted devices. Furthermore, electron mobility calculations of the electron only devices were carried out.

1.2 Literature Review

1.2.1 Electroluminescence

Electroluminescence (EL) is a phenomenon which semiconductor materials emit light due to passing electrical current or strong electrical field. EL occurs when electrons and holes are combined in semiconducting material. Emitting light is usually in visible range of electromagnetic spectrum (Figure 1.1). Because of same process can take place in infrared or ultraviolet section of electromagnetic spectrum, these emitted lights also called as EL. Constitutively, EL phenomenon consists of three main period: (a) providing electrical energy, (b) excitation process, (c) mechanism of emitting light.

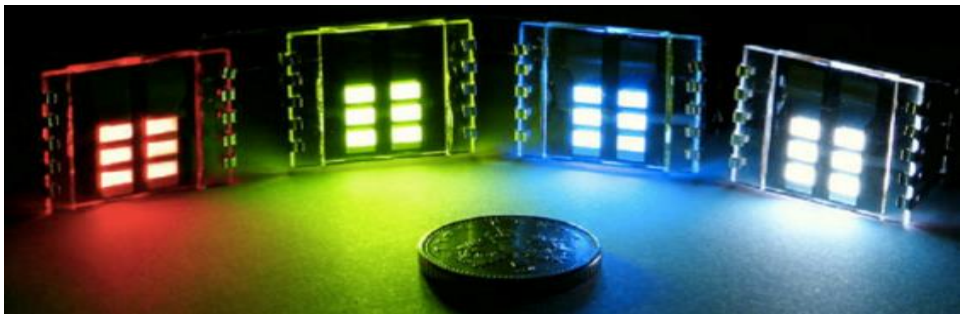

Figure 1.1 : Electroluminescent devices [5].

H.J. Round observed first electroluminescence occurrence in 1907 with a silicon carbide (SiC) compound. In the study, he observed yellow light while current is passing through a SiC detector [6]. The study was not repeatable until 1923 [7].

Between 1907 and 1923, no electroluminescent incident was reported. From this point, several electroluminescence studies could be seen in literature. In 1936, Destriau achieved to emit light from pulverulent zinc sulfide (ZnS) and Vlasenko and Popkov fabricated the first electroluminescent device based on ZnS. Moreover, they observed significant increase in electroluminescence in thin film form of zinc sulfide dopped with manganese [8,9].

Bernanose and his coworkers observed first organic EL by apply alternating current (AC) through acridine orange and quinacrine crystal thin film in 1953 [10]. Even though, first EL observed in organic materials in 1953, first current flow and detailed EL study was reported in 1963. In the research, when they applied high voltage (>100V) to anthracene thin film, which was produced by chemical method, they observed bright light [11].

In 1985, Ching Tang and Steven van Slyke fabricated a green light emitting OLED based on Alq_3. Since then, researches about OLEDs increased [1].

Two-layer OLED structure and EL spectrum is shown in Figure 1.2.

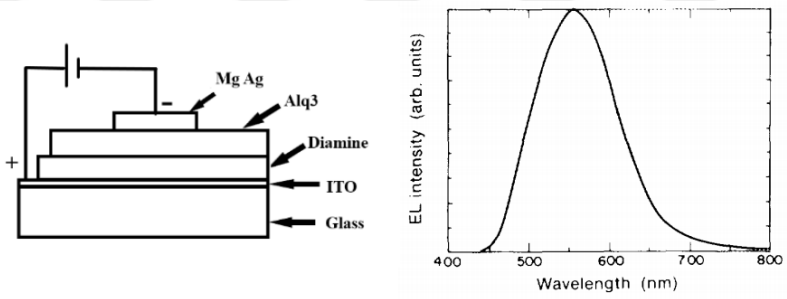

Figure 1.2 : Two-layer OLED structure and EL spectrum [12].

1.2.2 OLED types

Several types of OLEDs were produced until this day: passive-matrix OLED, active-matrix OLED, transparent OLED, top-emitting OLED, foldable OLED and inverted OLED. Each type of OLED has different application.

As shown in Figure 1.3, passive-matrix OLEDs (PMOLEDs) have strips of cathode, organic layer and strips of anode which is perpendicular to cathode. Each intersection of anode and cathode is a pixel of OLED. External circuit which turn on and off the pixels is required to apply current to electrodes. Brightness is proportional to applied

current. PMOLEDs are relatively easy to produce but they consume more energy than other OLED types because of their need for external circuit.

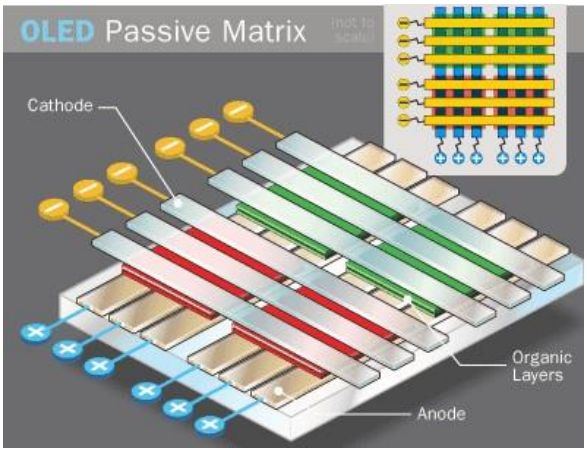

Figure 1.3 : PMOLED structure [13].

On the other hand, active-matrix OLEDs (AMOLED) have full layers of cathode, organic layers and anode with the difference of anode overlays a thin film transistor (TFT) array which forms a matrix. The TFT matrix is the circuit for OLED which consume less energy than an external circuit, so AMOLEDs are more efficient for large size displays (Figure 1.4).

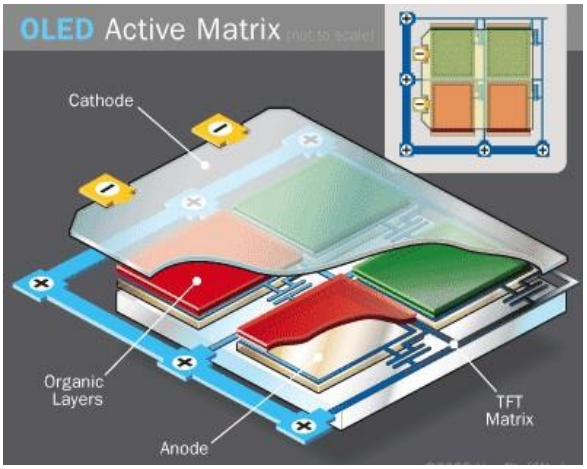

Figure 1.4 : AMOLED structure [13].

Transparent OLEDs (TOLEDs) have transparent layers of anode, cathode and organic layer onto transparent substrate, which leads 85% of transparency while OLED is turned off. Because both electrodes are transparent both sides of OLED can emit light and TOLEDs can be used as two-sided display. A TOLED can be either PMOLED or AMOLED.

Top-emitting OLEDs on the other hand, have either opaque of reflective substrate and they are suitable for AMOLED design because they can be easily integrated with non-transparent TFT.

Foldable OLEDs (FOLED) have very flexible substrate which are mostly plastic. FOLEDs are very lightweight and durable. Their usage prevents breakage of screens and major damages. FOLEDs have very potential usage such as smart clothing.

Inverted OLEDs have opposite charge transport mechanism of conventional OLEDs. For conventional OLED devices, cathode is situated on top of device. On the other hand, for inverted OLEDs cathode is at the bottom of device. Since TFTs are mostly n-type, inverted OLEDs with a bottom cathode are preferred for AMOLED devices. A detailed information about inverted OLEDs are given in section 1.2.4.

1.2.3 OLED materials and coating methods

Advantages of organic materials are high luminescence and variety of colors. Light in organic materials is generated due to fast turn back to ground state of excited molecules and color of the emitted light is associated with energy difference of ground state and excited state.

Organic semiconductors have various physical properties which provide many advantages; a) some organic dyes have high absorption efficiency within visible region which make them very convenient candidate for very thin photodetector and photovoltaic cell applications [14], b) Stokes shift is relatively high for many luminescent dyes which minimize losses such as reabsorption [12], c) almost infinitely many chemical materials and ability of synthesis situational materials ensure diversity, d) organic semiconductors mostly coat in room temperatures and they suit with foldable substrate.

Several organic materials are capable of transport both electrons and holes. Electron and hole mobilities are range between 10^{-8} and 10^{-2} $cm^2/(V\ s)$ in organic materials and electron mobility usually less than hole mobility [15]. For example, Alq_3 is an electron transport material and its electron mobility is 100 times larger than its hole mobility [16].

There are various methods to coat an organic material; Vacuum evaporation method is most used method for coating small molecules. For coating large surfaces, organic

vapor phase deposition (OVPD) is more suitable method [17]. Apart from these, spin coating, inkjet printing, screen printing, drop casting or dip coating methods can be used for soluble organic materials or polymer materials.

1.2.4 Device structure

Simplest conventional OLED design is one-layer structure. This structure consists of indium tin oxide (ITO) is coated as anode electrode onto glass or plastic substrate, top of that organic emissive layer is coated, and finally metal cathode electrode is deposited with vacuum evaporation method. However, this structure is not suitable for efficient OLED fabrication. For low voltage and high efficiency, at least two organic layers are preferred mostly.

In two-layer conventional structure, there are several layers which are; anode, hole transport layer (HTL), electron transport layer (ETL) and cathode. ITO as anode is used for hole injection and it is transparent for allow the light transmission. Metals with low work function such as Al, Mg, Ca etc. are used for electron injection as cathode. HTL is responsible for hole transportation from ITO to organic interlayer on the other side, ETL is responsible for electron transportation from cathode to interlayer. If recombination zone (emission layer, EML) is in ETL, ETL act as EML otherwise HTL act as EML. So, these devices can be categorized as two different structures; Anode/HTL/ETL(EML)/Cathode or Anode/HTL(EML)/ETL/Cathode. Besides, EML can be coated between HTL and ETL individually for fabricate three-layer structure (Anode/HTL/EML/ETL/Cathode). Conventional device structures can be seen in Figure 1.5.

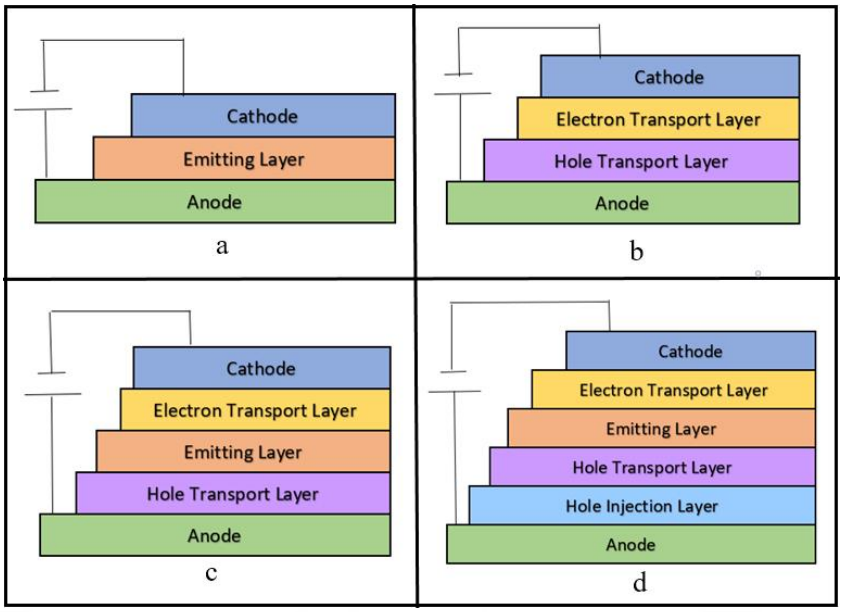

Figure 1.5 : Conventional OLED structures; a) one-layer OLED, b) two-layer OLED, c) three-layer OLED, d) multi-layer OLED.

It is found that inserting a hole injection layer (HIL) between ITO and HTL decreases the required voltage, increases the efficiency of device. Because of the interaction between ITO and organic layer can cause degradation of device, HIL also enhance the device stability [18,19]. Same situation occurs for interlayer between metal cathode and organic layer. Used injection layer thickness depends on resistance of the material. For high resistant materials thickness is usually less than 10 nm and for some doped injection layers thickness reaches up to 100 nm [20,21]

As mentioned before, in conventional OLED structure, metals with low work function are used as cathodes. Because of their low work function, these metals are very sensitive to oxygen and moisture. Conventional device structure (low work function top cathode) restricts the fabrication of device in atmospheric conditions and causes rapid degradation. In inverted OLED structure the charge motion is exact opposite of conventional structure. Bottom electrode (ITO) becomes cathode and higher work function (more stable) top electrode becomes anode (Figure 1.6). Besides, metal oxide materials such as ZrO_2, TiO_2 and ZnO are used as electron injection layer (EIL) and V_2O_5, WO_3 and MoO_3 are used as hole injection layer (HIL) [22-25]. These materials cause intrinsic encapsulation due to their high oxygen and moisture absorbent properties and provide environmental stability [26,27]. Also, PEDOT:PSS is unstable hole injection material which used widely for conventional devices. Hence, avoid using PEDOT:PSS in inverted devices increases the life time.

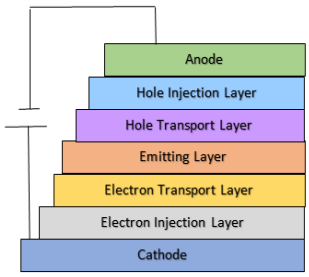

Figure 1.6 : Inverted OLED structure.

1.2.4.1 Hole injection/transport materials

In OLED systems, thin films like copper (II) phthalocyanine (CuPc) [18], SiO_2 [28] are used for improving hole injection. In addition to this, materials such as $FeCl_3$ doped with oxidizing agent [29], iodine [30], tetrafluorotetracyano-quinodimethan (F4-TCNQ) [31] is used. In hibrit OLED systems mostly used HIL is poly(3,4-ethylenedioxythiophene)-poly(styrenesulfonate) (PEDOT:PSS) [32-34]. PEDOT:PSS is a water based solvent and it smooths the surface of ITO, prevents possible electrical short-circuit, decreases required voltage [35].

N,N′-Bis(3-methylphenyl)-N,N′-diphenylbenzidine (TPD), derivative of aromatic diamine is a typical hole transport material [36-38]. It has high hole injection, hole transport and electron blocking properties. Even if it has prior properties as hole transport material, when it is deposited with vacuum evaporation its thermal stability is relatively low because of low glass transition temperature (T_g= 63 °C). On the other hand, (N,N′-di(naphthalene-1-yl)-N,N′-diphenyl-benzidine (NPB) and Poly(9-vinylcarbazole) (PVK) is another mostly used hole transport material [18, 39-40]. Hole mobility of hole transport materials are generally range between 10^{-3} and 10^{-4} $cm^2/(V\ s)$. Total current in OLEDs is determined by hole transport materials because of their efficient hole transport properties and high hole transport rate. Examples of molecular structure of hole injection and hole transport materials is shown in Figure 1.7.

A good hole transport/injection material should have these features;

- Morphologically stable
- Low ionization potential,
- High hole mobility,
- Low electron attraction.

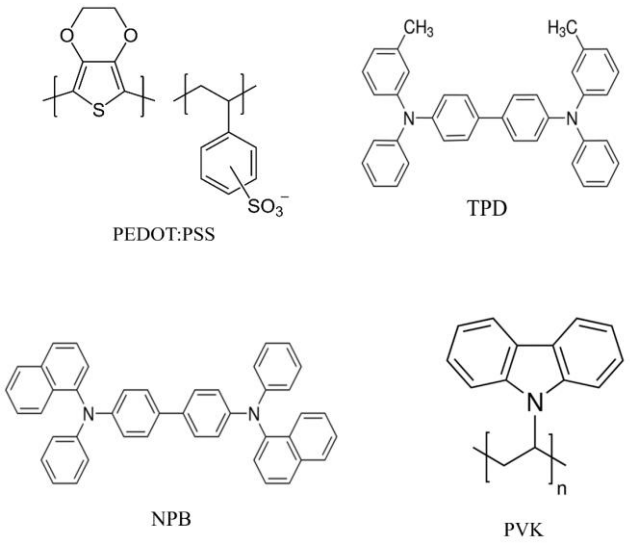

Figure 1.7 : Examples of hole injection and hole transport materials.

1.2.4.2 Electron transport materials

One of the most known electron transport material is Alq_3 (Tris-(8-hydroxyquinoline)aluminum). Its electron mobility depends on electrical field and its value is approximately 10^{-6} $cm^2/(V\ s)$ at 4 x 10^5 V/cm. Alq_3 is also used as emissive material and it emits green light around 530 nm wavelength [41].

Bathocuproine (BCP) [42,43], 3-(Biphenyl-4-yl)-5-(4-*tert*-butylphenyl)-4-phenyl-4*H*-1,2,4-triazole (TAZ) [44], Bis(8-hydroxy-2-methylquinoline)-(4-phenylphenoxy)aluminum (BAlq) [45] and 2,2′,2"-(1,3,5-Benzinetriyl)-tris(1-phenyl-1-H-benzimidazole) (TPBi) [46-48] are other mostly used electron transport materials. Examples of molecular structure of electron transport materials is shown in Figure 1.8.

A good electron transport material should have these features;

- Morphologically stable
- High ionization potential,
- High electron mobility,
- High electron attraction.

.

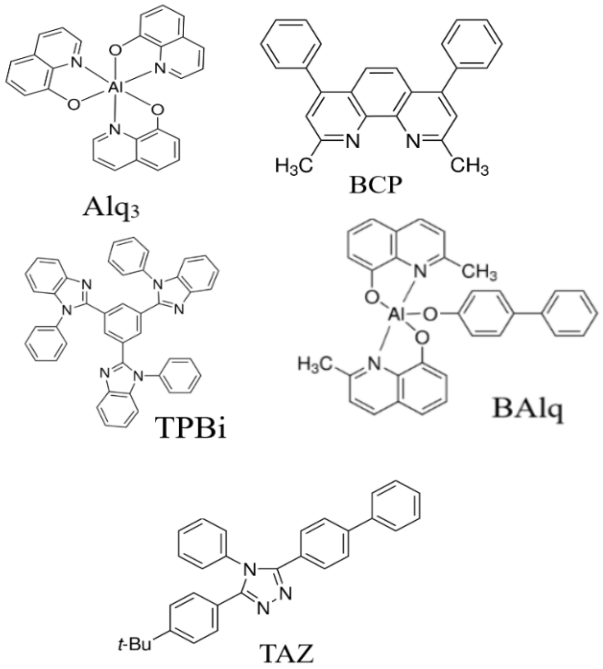

Figure 1.8 : Examples of electron transport materials.

1.2.4.3 Emissive materials

Many luminescent materials with high quantum efficiency are used in OLEDs as emissive layer. However, just a few of them show strong emissive layer characteristics. There are two main types of OLEDs according to the used emissive material;

a) PLEDs; which include EL polymers for light emitting process. Usually polymeric emissive materials are soluble, and solution processed (i.e. spin-coating) while device fabrication.

b) SMOLEDs; which contain small molecules in order to emit light. Usually small molecules are not soluble, and vacuum deposited during device fabrication.

Pioneer researches about EL polymers and their devices was based on PVK (poly(N-vinyl carbazole) and doped with several luminescent dyes [49,50]. Burroughes and his coworkers introduced electroluminescent polymers in 1990 that describes an EL device based on conjugated poly(p-phenylene vinylene) (PPV) [51]. PPV is highly stable conjugated polymer and it has yellow fluorescence around 400-420 nm [52-58]. Since 1990, PPV polymers drew tremendous attention and its numerous derivates synthesized. MEH-PPV (Poly[2-methoxy-5-(2-ethylhexyloxy)-1,4-phenylenevinylene]) is one of the best known EL polymer.

Polyfluorenes are EL polymers which can be used in PLEDs as well. They have great optical and electronic properties and high stability. Fluorene (Fl) is a polycyclic aromatic compound which has strong violet fluorescence. As a matter of fact, polyfluorenes are the only class of conjugated polymers that emit a whole range of colors [59-65]. [Poly[9,9-didodecylfluroenyl-2,7-yleneethylnylene] is one of the examples of polyfluorenes.

Commonly used emissive small molecules are iridium complexes and first used iridium complex was fac tris(2-phenylpyridine) iridium ($Ir(ppy)_3$) complex [66]. Even they have relatively high phosphorescent efficiency, in solid state, iridium complexes are not very efficient due to aggregation tendency. Therefore, usually these materials are used as dopants in a host medium to decrease aggregation. Tris[2-(4-*n*-hexylphenyl)quinoline)]iridium(III) (Hex-Ir(piq)$_3$) and Bis(3,5-difluoro-2-(2-pyridyl)phenyl-(2-carboxypyridyl)iridium(III) (FIrPic) are another known iridium complexes. Examples of emissive layer materials both polymers and small molecules are shown in Figure 1.9.

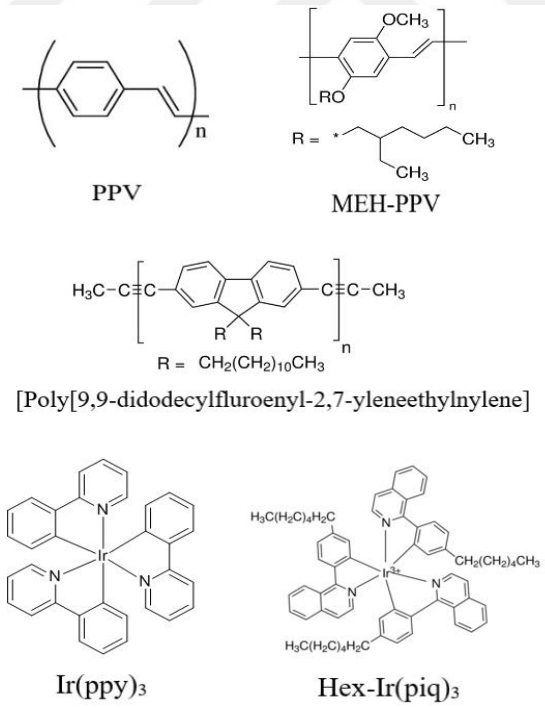

Figure 1.9 : Example of emissive materials.

1.2.4.4 Anode materials

In an OLED device, fundamental factor which determine the hole injection is difference between work function of anode and ionization energy of organic

material. For a convenient charge transfer, anode should have high ionization potential.

Because of the high transparency (>85%) and low resistance, ITO is most preferred anode material. ITO substrates are made by coating indium oxide (In_2O_3)/ tin oxide (SnO_2) onto plane glass substrate by sputtering.

Cui and his coworkers found 4 alternative high transparent, conductive oxide materials which can be used as anode materials. These are $Ga_{0.12}In_{1.88}O_3$ (GIO), $Ga_{0.08}In_{1.28}Sn_{0.64}O_3$(GITO), $Zn_{0.5}In_{1.5}O_3$ (ZIO) and $Zn_{0.46}In_{0.88}Sn_{0.66}O_3$ (ZITO) [67]

Due to its brittle structure, ITO is not suitable for flexible OLED production. For this reason, the search for anode to adapt to flexible substrate continues. Therefore, studies on using graphene instead of ITO are ongoing [68-70].

1.2.4.5 Cathode materials

The primary carriers in OLED systems are the holes because of their hole mobility and low barrier difference. Therefore, decreasing energy barrier for electron transfer is essential. Thus, more efficient recombination and increased luminescence is achieved by increasing ratio of electrons and holes in organic material. Hence, metal cathodes with low work function are preferred.

Mg:Ag alloy is one of the most preferred cathode material due to its low work function. Adding silver is increased chemical stability of magnesium and avoids leakage of magnesium into lower levels [71]. Al, Ag and Au are other mostly used metals for cathode, also for inverted device structure, ITO becomes cathode instead of anode, mainly because increase environmental stability and increase electron injection.

Adding a very thin layer of LiF between Alq_3 and Al, increase electron injection efficiency [72]. LiF thin layer was used various OLED systems. For example, a blue OLED with LiF/Al cathode has 1.4% external quantum efficiency and 50 times higher efficiency with respect to standard OLED without LiF [73]. Likewise, another OLED device with just Mg:Ag cathode showed very low luminescence at 15V. On the other hand, after adding LiF thin layer, device showed superior improvements in terms of both luminescence and efficiency [74].

1.2.5 Working principle of OLEDs

When an external current is applied to an OLED device, electrons are injected from cathode and holes are injected from anode. After that, these electrons and holes passing through organic layers via hopping process and reach to emissive layer. In this layer electrons and holes recombine by effect of electrostatic forces and forming exciton, which is a bound state of the electron and hole. Outcome of this exciton's decay is relaxation of the energy and this energy emits radiation in visible region. The frequency of this radiation depends on the energy difference between HOMO (highest occupied molecular orbital) and LUMO (lowest unoccupied molecular orbital) of the material. In Figure 1.10 working principle of a simple OLED is shown.

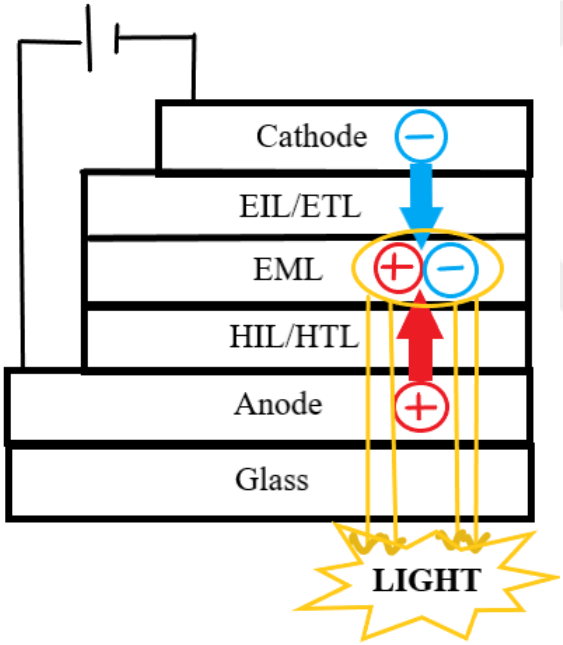

Figure 1.10 : Working principle of OLED.

1.2.6 Device physics

Most significant difference between organic and inorganic light emitting diodes are charge injection and transfer mechanism. In inorganic LEDs charge injection rely on pn-junction. On the other hand, in organic LEDs charges are injected from electrodes. However, charge mobility in organic materials is relatively low because of overlap orbitals due to the weak van-der-waals interaction. After all, voltage and charge conditions for organic LEDs and inorganic LEDs are very different. In inorganic LEDs, charge density is almost constant outside junction region. But, in

organic LEDs, charges gather around electrodes and while steer away from electrodes charge density is decreased (space-charge limited region).

After injection of charges, near electrodes, space-charge regions occur and therefore, net charge density decreases while moving away from contacts. As shown in Figure 1.11, two layered OLED with suitable energy levels, injected charges are stopped by interlayers. Recombination of opposite charges occurs near these interlayers [75].

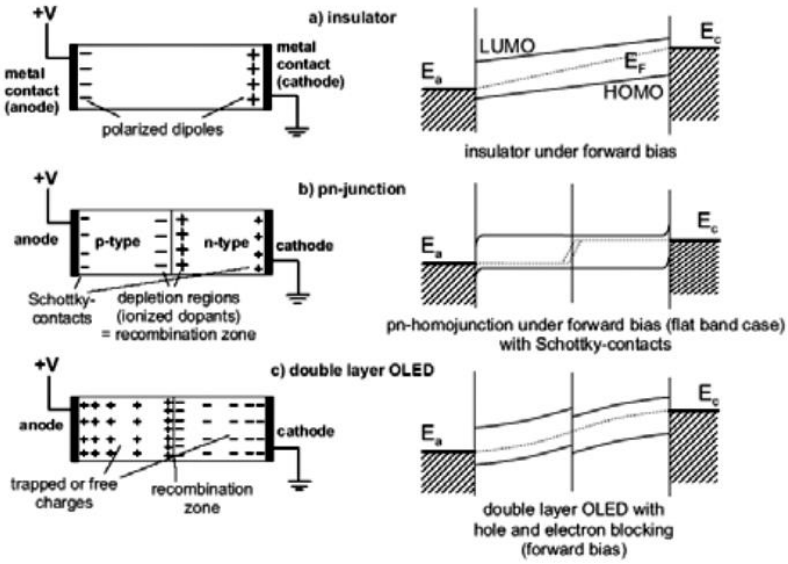

Figure 1.11 : a) insulator, b) inorganic p-n junction and c) double layer OLED's net charge density (left) and energy level differences (right).

1.2.6.1 Charge transfer

In order to achieve high efficiency (emitted photon for each electron), every layer should have specific properties. HIL should transfer holes easily from anode to hole transport layer. This can be achieved when transport layer's HOMO is in between ITO's ionization potential and emissive layer's HOMO. At the same time, HTL should have high hole mobility and block electrons to reach anode which come from cathode.

Emissive layer's HOMO and LUMO energy levels should be suitable for transporting charges from neighbor layers. Likewise, EIL and ETL's HOMO and LUMO levels should be suitable and these layers should have high hole mobility as well.

Most organic material has dominantly n- or p- type conductivity by itself. Today, many methods are used to increase conductivity and charge density i.e. doping. In

addition to doping, morphology and thickness of thin film layers are very crucial for charge transfer properties. Optimum thickness of organic layers should be chosen for blocking electrons and holes to reach opposite electrodes.

1.2.6.2 Recombination

After injecting electrons and holes from opposite electrodes, they reach to emissive layer via injection and transport layers. The region where electrons and holes recombine and emit light is called recombination zone and this zone is only a few nm thickness.

Electrons and holes are fermions with half integer spin. Based on the relative orientation of two spins, the exciton can either have a total spin of zero or a total spin of one which are called singlet and triplet exciton, respectively. There are three combinations which form a triplet exciton and only one combination that form singlet exciton. Hence, 75% of the formed excitons are triplet and 25% of the excitons are singlet (Figure 1.12).

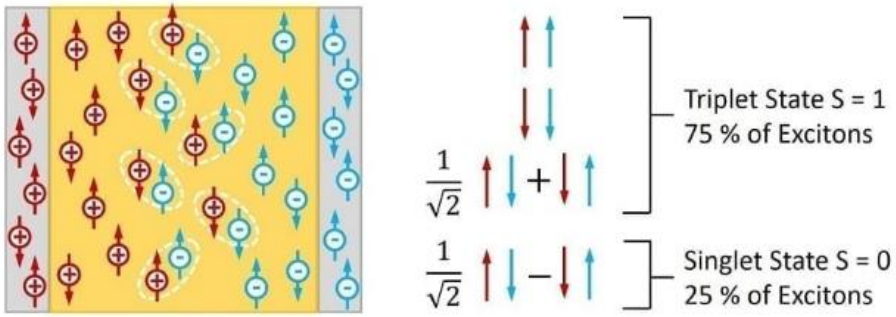

Figure 1.12 : Schematic representation of singlet and triplet state.

On behalf of achieving high efficiency, emissive layer's photoluminescence efficiency (ratio between recombined excitons and consisted excitons) should be high and Stokes shift must be great. Stokes shift is unique property for each emissive material. Stokes shift of molecule synthesized by Li and coworkers was found to be as large as 325 nm [76].

1.2.6.3 Exciton diffusion and annihilation

Excitation energy is transferable to other molecules with same or lower excitation energy. This process is explained by Dexter and Förster energy transfer mechanisms.

Diffusion length of singlet exciton is found to be between 4-25 nm in various researches [77-80]. Combinations without emitting light only occur in electrodes or when there is an impurity in emissive material. Contact annihilation can be avoided by trapping excitons in emission layer via using transport layers with higher singlet exciton energy (Figure1.13).

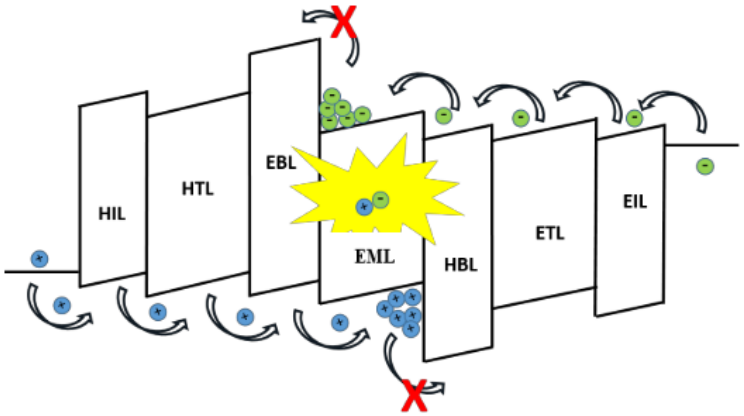

Figure 1.13 : Energy level diagram of OLED.

1.2.7 Doping in OLEDs

Key progress which led to improve OLED technology is discovery of doping [71]. Conjugated organic semiconductors usually do not contain pure and free charges. Therewithal, many organic semiconductors have high mobility for only one type charge (hole or electron). Hence, while designing OLED device, it is possible to choose materials with unique mobility characteristics.

The main goal of doping is obtain high efficiency by using host material with optimized mobility and luminescence properties mixed with guest material with high luminescence. Most important benefit of doping is increase working stability of OLED by decreasing passing time without emitting light [81]. In addition to this, it is almost impossible to predict doping effect by taking into consideration of energy levels. Many other internal or external parameters may affect doping efficiency.

Controlled and stable doping is preferable for improving efficiency of many organic based devices. If fermi energy levels of organic semiconductors could shift to mobility level, ohmic losses would decrease and it would be easy to inject charges from electrodes. Baldo and his coworkers achieve to increase internal EL efficiency of OLED up to 100% by doping phosphorescence materials [82].

1.2.8 Device characterization

In this section characterization methods and equipments are explained which were used in this thesis.

Hamamatsu PMA-12C10027 Photonic Multichannel Analyzer (C9920-11, integrated with 2427-C3A Keithley) is used for examination of luminescence (cd m^{-2}) , passing current (A), CIE color coordinates, current density (mA cm^{-2}), external quantum efficiency (%), current efficiency (cd A^{-1}) and power efficiency (lm W^{-1}). Measuring system is shown in Figure 1.14.

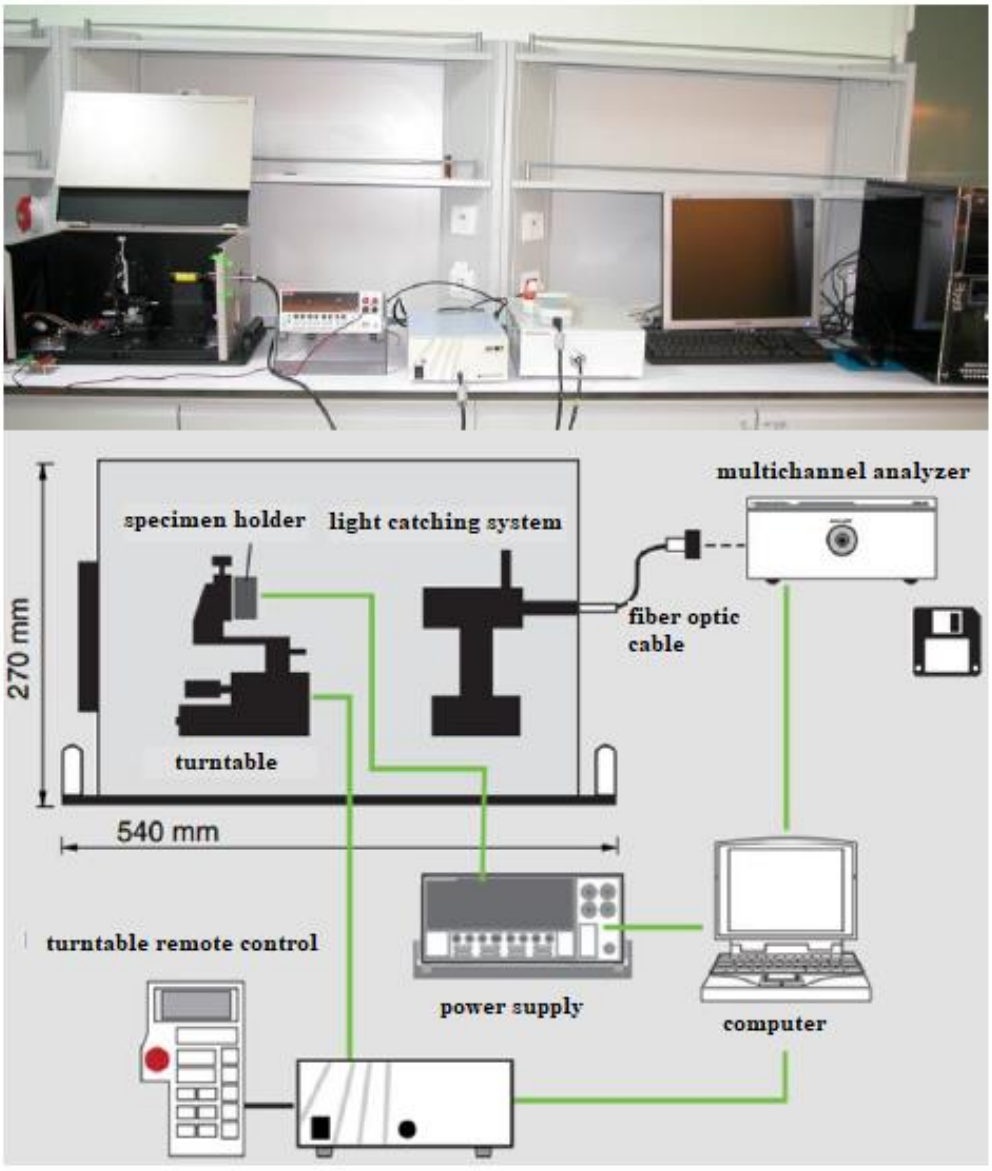

Figure 1.14 : Characterization system and schematic diagram.

Color of OLED emission is characterized by CIE 1931 XYZ standard (Figure 1.15). CIE 1931 XYZ color standard is defined by x(λ), y(λ), z(λ). Human eye has three photoreceptor cells which sense light (correspond to long, middle, short wavelength), for this reason, color perception is possible with three values;

$$X = \int I(\lambda)\bar{x}(\lambda)d\lambda \quad \textbf{(1.1)}$$

$$Y = \int I(\lambda)\bar{y}(\lambda)d\lambda \quad \textbf{(1.2)}$$

$$Z = \int I(\lambda)\bar{z}(\lambda)d\lambda \quad \textbf{(1.3)}$$

Where I(λ) is emission spectrum. In this study, CIE color coordinates were reported with xyY formulation of 1931 color standard (Figure 1.16). Advantage of this method is specifying color with only 2 variables by distinguishing color and luminescence.

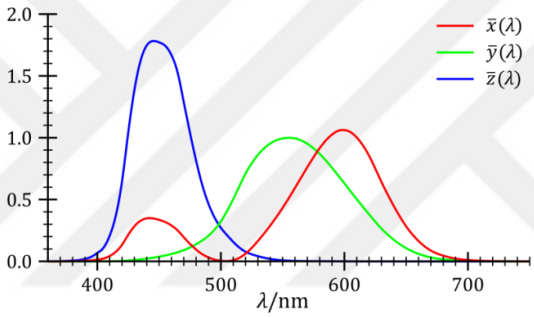

Figure 1.15 : The CIE XYZ standard observer color matching functions.

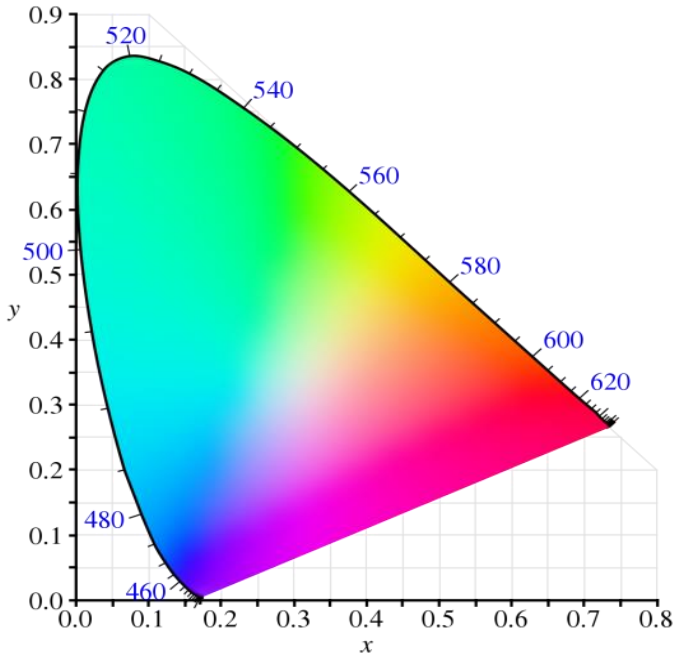

Figure 1.16 : Characteristic CIE xyY color standard spectrum.

External quantum efficiency (EQE) is simply ratio between number of photons emitted from device and number of injected electrons to device. EQE is calculated by equation 1.4;

$$\eta_{ext} = \frac{\iint \frac{F_{abs}(\lambda,\theta)}{\hbar c/\lambda} d\theta d\lambda}{I/e} = \frac{N_p}{N_e} \quad \textbf{(1.4)}$$

Where, ∫ Fabs(λ,θ)dθ is total emission, λ is wavelength, θ is measurement angle, $\hbar$ is plank constant, c is speed of light, I is current and e is the charge of an electron.

2. EXPERIMENTAL DETAILS

2.1 Materials

In order to fabricate red light emitting OLED, Hex-Ir(piq)$_3$ phosphorescent material was chosen because of its emitted color and potential applications in display technology. Although, there are several researches about this small molecule, very limited resources were found about solution processed Hex-Ir(piq)$_3$ in literature [83-85]. Different host materials were tried for performance improvements in various device structures.

Several polymers, small molecules, metal and metal oxides were used in this contribution. MEH-PPV (M_n: 40000-70000 - 541443-1G), NPB (sublimed grade, 99% - 556696-1G), PVK (M_w ~1,100,000, powder - 182605-5G), TPD (99% - 443263-5G) and LiF (≥99.99% trace metals basis - 449903-2G) were purchased from Aldrich. Hex-Ir(piq)$_3$ (> 99% - LT-N754) and TPBi (Sublimed, > 99.5% - LT-E302) were purchased from Lumtec. Ca (99% - EVMCAX203MMD) and Al (99,999% - EVMAL50QXQ-J) pellets for thermal evaporation were purchased from Kurt J. Lesker. V_2O_5 (99.99%, metals basis – 10904.09) was purchased from Alfa Aesar, and PEDOT:PSS (CLEVIOS™ P VP AI 4083) was purchased from Heraeus. For inverted OLEDs, ZnO:PEI binary nano-composite (BNC) and ZnO:PEI:TPBi ternary nano-composite (TNC) were synthesized as specified [2,86]. ZnO particles were synthesized with chemical precipitation method by using zinc acetate dihydrate ($Zn(CH_3COO)_2 \cdot 2H_2O$; ≥ 99.0 %, Aldrich) and potassium hydroxide (KOH; ≥ 99.0 %, Aldrich). Sedimented by centrifugation ZnO particles dispersed in 50% diluted polyethylenimine (PEI, M_n: 60 000, Across Organics) in order to prepare binary nano-composite (BNC). Trace quantity of TPBi were disperse into BNC solution to prepare ternary nano-composite (TNC). All chemicals were used without additional purification.

2.2 Device Fabrication

2.2.1 Substrate preparation

In order to fabricate OLED devices 1×1 inch ITO coated glass substrates (120 nm, 15Ω/sq, patterned) were provided from Kintec Company. ITO coated glass substrates were cleaned in acetone, detergent (PCC-4, 2% wt. dispersed in water), deionized water and isopropyl alcohol by ultrasonication for 15 minutes each and dried under N_2 (nitrogen) gas flow. Afterwards, the substrates were exposed to oxygen plasma for 5 minutes for remove all organic impurities. Schematic of chemical cleaning process and oxygen plasma system are shown in Figure 2.1.

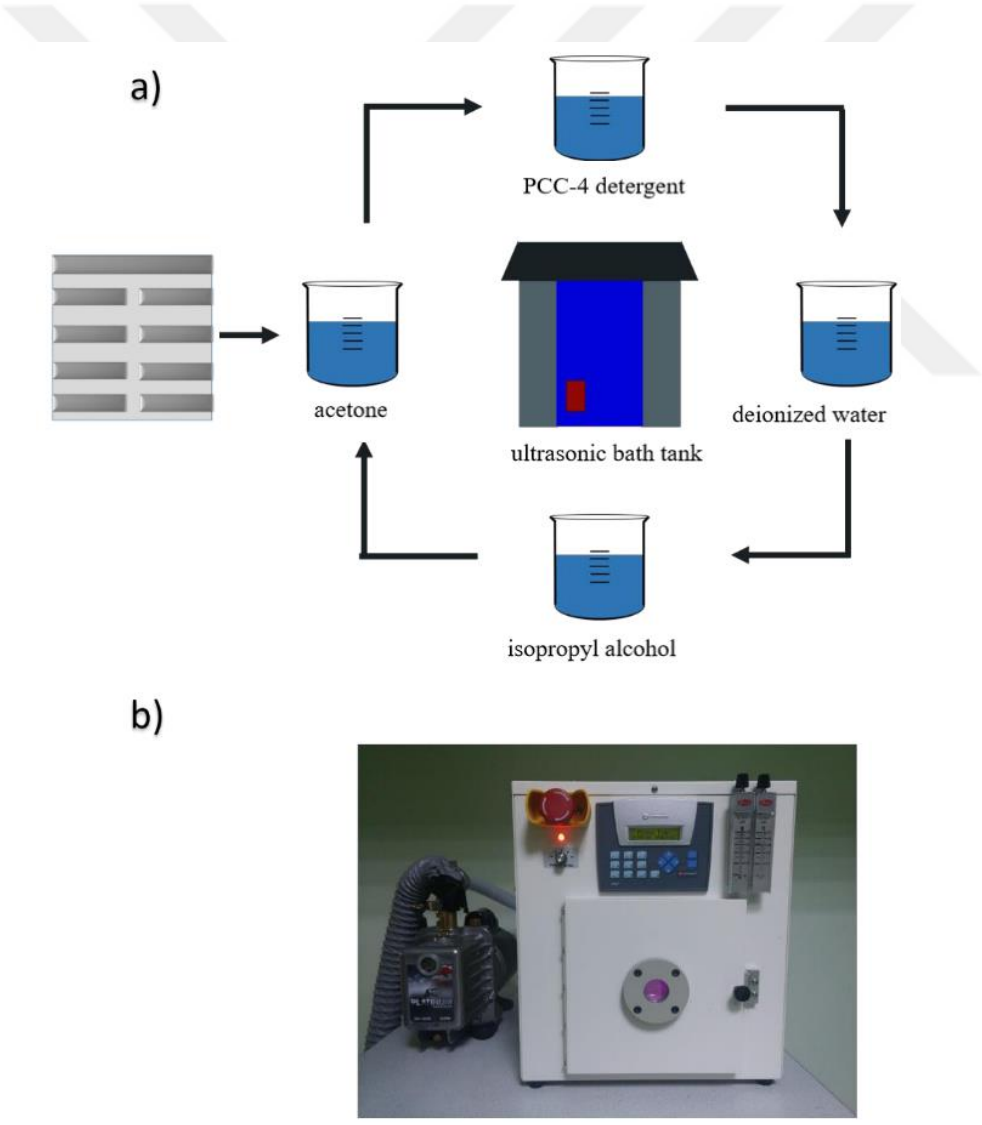

Figure 2.1 : Schematic representation of ITO substrate and chemical cleaning process of ITO substrate b) oxygen plasma system.

2.2.2 Growing functional layers

In order to fabricate conventional OLEDs, PEDOT: PSS solution was spin-coated at 3000 rpm for 30 seconds and annealed at 120℃ for 20 minutes in ambient air as HIL. Subsequently, Hex-Ir(piq)$_3$ solutions with different dopant ratios and hosts were spin-coated at different spin rates for 50 seconds and annealed at 120℃ for 10 minutes in glove-box system as emissive layer. 1:3 dichlorobenzene (DCB), toluene mixture was used as solvent for all Hex-Ir(piq)$_3$ solutions and all solutions were filtered through a 0.45μm membrane filter (Milipore PTFE) before coating. Schematic representation of spin-coating method is shown in Figure 2.2. TPBi as ETL was deposited with thickness of 10 nm in a vacuum evaporator (2×10^{-6} mbar), which is integrated in glove-box system. The devices were completed by the deposition of Ca (10 nm) as EIL and Al (100 nm) as cathode layer in another vacuum evaporator (2×10^{-6} mbar) in order to avoid organic impurities from other vacuum evaporator.

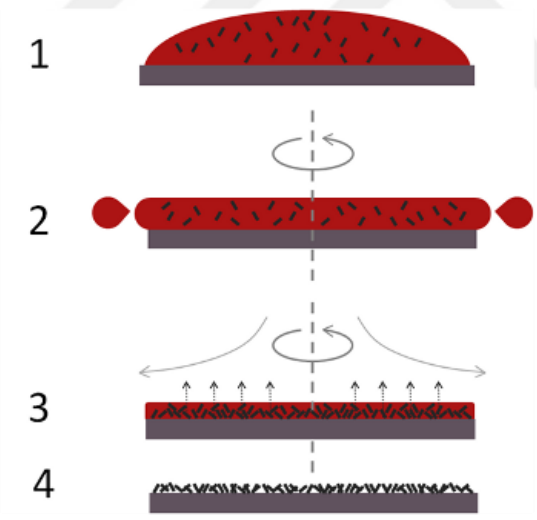

Figure 2.2 : Schematic representation of spin-coating method.

BNC or TNC solution was spin coated at 2500 rpm for 30 seconds and cured at 120℃ for 120 minutes in ambient air as EIL for fabrication of inverted OLEDs. Following by the same emissive layer coating procedure as conventional OLEDs. TPD (50 nm) was deposited in first vacuum evaporator as HTL afterward, V_2O_5 (15 nm) as HIL and Al (100 nm) as cathode were deposited in second vacuum evaporator. Glove-box system used for fabrication is shown in Figure 2.3.

Figure 2.3 : Glove-box system which used for device fabrication.

Finally, in order to fabricate e-only devices 1×1 inch glass substrates were cleaned with same cleaning process of ITO coated glass substrates which mentioned before. Al was deposited as anode with the thickness of 100 nm onto substrate in vacuum evaporator. Host free Hex-Ir(piq)$_3$ and Hex-Ir(piq)$_3$ doped solutions were spin-coated at 1500 rpm for 50 seconds and cured at 120°C for 10 minutes. Subsequently, the devices were transferred to vacuum evaporator once again and LiF (1 nm) as EIL and Al (100 nm) as cathode were deposited at 2×10^{-6} mbar. All fabricated device structures are shown in Figure 2.4.

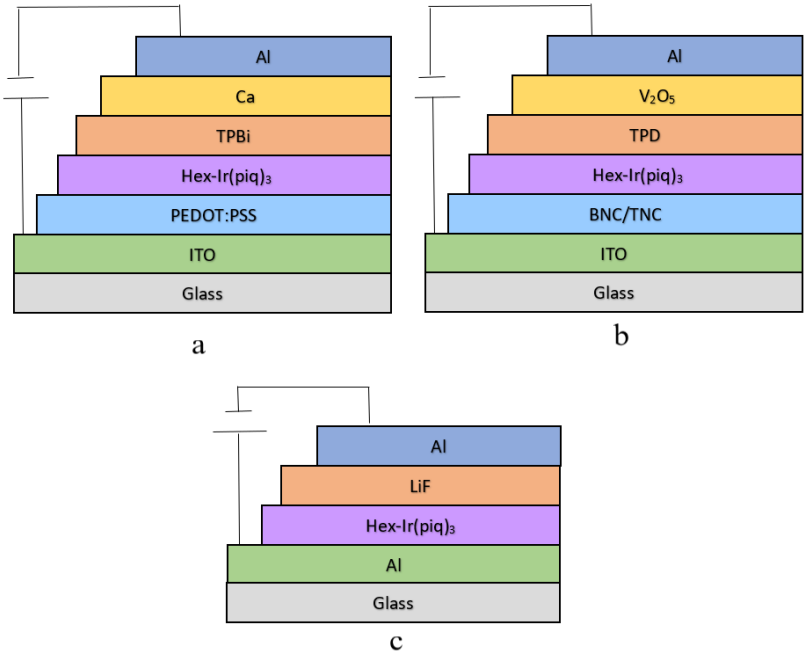

Figure 2.4 : Fabricated device structures a) conventional OLED b) inverted OLED c) e-only device.

2.2.3 Encapsulation

Oxygen and moisture sensitivity of functional layers affect stability and lifetime of devices. Therefore, in order to minimize atmospheric exposure different methods can be used. One of the mostly used encapsulation method is attach glass with UV sensitive resin. Alternatively, atomic layer deposition (ALD) method is becoming popular recently. Because of its practicality, encapsulation bands (Adhesives Research, EL-92734) were used in this study. After encapsulation, devices were taken out of the glove-box and then characterized.

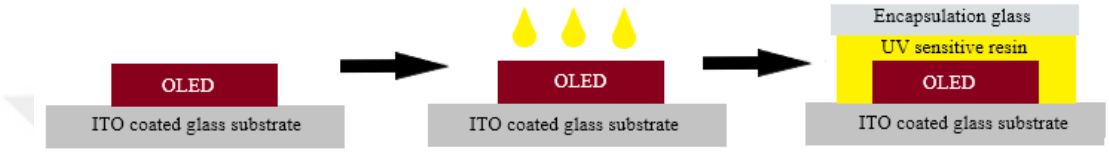

Figure 2.5 : Schematic representation of glass encapsulation process.

3. RESULTS AND DISCUSSION

3.1 Electrical and Optical Characterization Results

Firstly, solution of Hex-Ir(piq)$_3$ without host were prepared for understanding the performance characteristics of the molecule itself. Conventional and inverted devices were fabricated with various thickness of Hex-Ir(piq)$_3$ and the effect of thickness on the device performances were examined. For both conventional and inverted devices concentration of Hex-Ir(piq)$_3$ solution was chosen 10 mg/ml and after spin coating process coated thin films were cured at 120℃ for 10 minutes.

In Figure 3.1, electrical and optical characterization of conventional no host Hex-Ir(piq)$_3$ devices were shown. Four different spin coating rates (1000 rpm, 1500 rpm, 2000 rpm and 2500 rpm) of Hex-Ir(piq)$_3$ layer were chosen to find optimal spin rate. Fabricated conventional OLED structure was ITO / PEDOT:PSS / Hex-Ir(piq)$_3$ / TPBi / Ca / Al. Even though, fabricated device with 1000 rpm spin rate gave a high efficiency, thin film of this layer had morphological defects which could be seen with naked eye. These defects lead to black spots and inhomogeneous light emission in OLED as shown in Figure 3.2. This might be because of poor thin film quality of small molecules from solutions and 1000 rpm might not be enough to obtain homogeneous thin film. Therefore, the optimum spin rate was determined as 2500 rpm for this device structure in terms of thin film quality and emitted light stability.

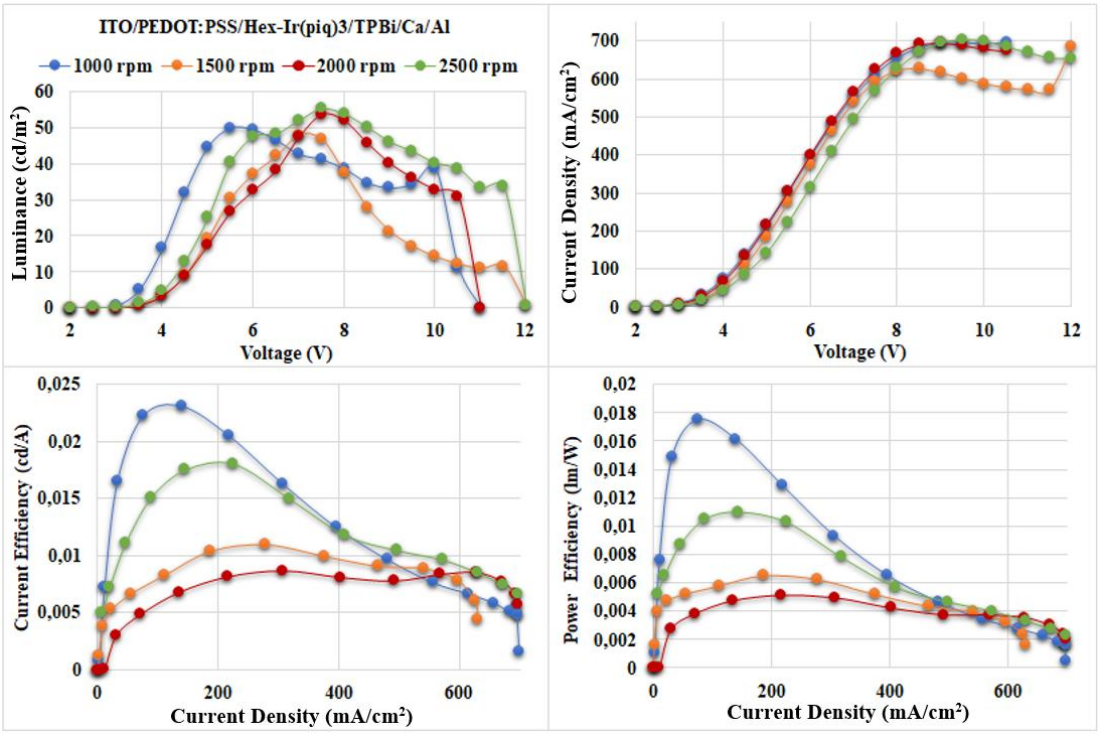

Figure 3.1 : Characterization of conventional host free Hex-Ir(piq)3 devices.

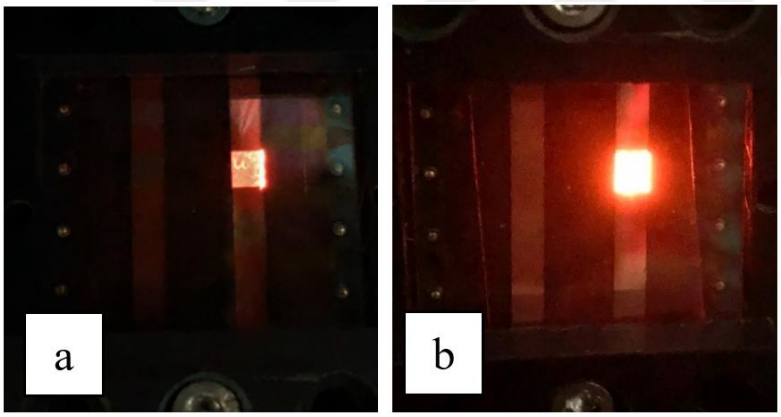

Figure 3.2 : a) Morphological defects resulted in inhomogeneous light emission, b) homogenous light emission.

Spin rates for inverted OLEDs were chosen as 2000 rpm, 2500 rpm and 3000 rpm because of the resulted poor film qualities of fabricated conventional OLEDs with 1000 and 1500 rpm spin rate. Fabricated inverted OLED structure was ITO / BNC / Hex-Ir(piq)$_3$ / V_2O_5 /Al. Electrical and optical characteristics of inverted OLEDs were shown in Figure 3.3. As seen in Figure 3.3, the optimal spin rate was found to be 2500 rpm for inverted Hex-Ir(piq)$_3$ only device, same as conventional.

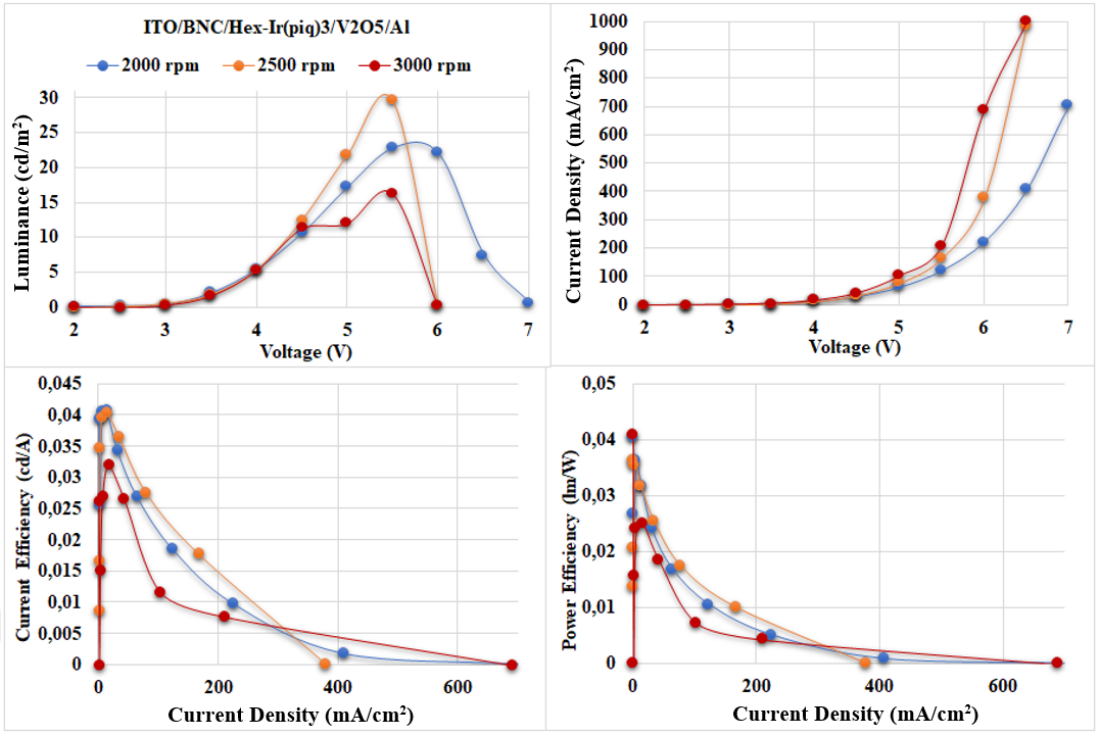

Figure 3.3 : Characterization of inverted host free Hex-Ir(piq)$_3$ devices.

In addition, effect of adding a TPD thin film layer as hole transport layer and using TNC (ternary nano-composite, ZnO:PEI:TPBi) instead of BNC (binary ZnO nano-composite, ZnO:PEI) for inverted device structure was studied (Figure 3.4). OLED devices were fabricated as ITO / BNC / Hex-Ir(piq)$_3$ / TPD / V_2O_5 /Al and was ITO / TNC / Hex-Ir(piq)$_3$ / TPD / V_2O_5 /Al, respectively. For both devices spin coating rate was chosen as 2500 rpm.

As seen in Table 3.1, addition of TPD layer was made great improvement to device performance. Luminescence value was increase from 29 cd/m^2 to 370 cd/m^2 and external quantum efficiency was increased from 0.06% to 0.9% which showed hole transport is a key factor for this molecule. This may be the reason behind the relatively low efficient for conventional OLED. Additional hole transport layer may require for this structure, as well. However, because of the process was solution based, additional hole transport layer may dissolve in DCB, toluene or water which cause catastrophic results while coating itself or top layer.

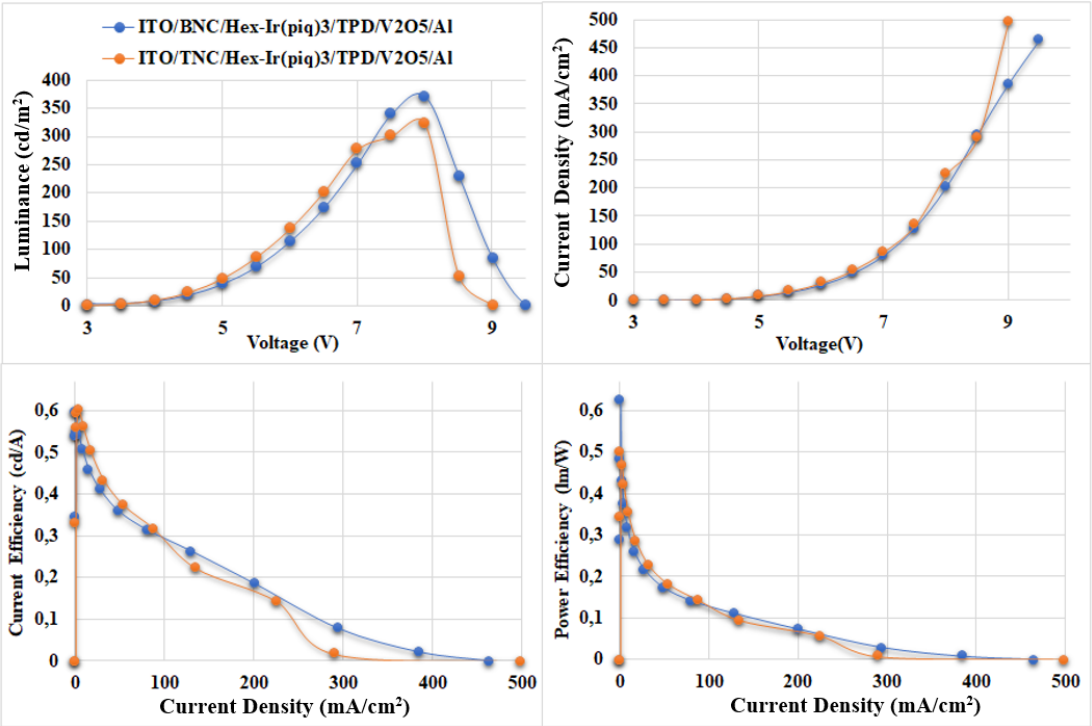

Figure 3.4 : Comparison of using BNC and TNC.

Furthermore, using BNC was slightly more efficient than TNC. These solutions were dispersed ZnO particles in PEI (polyethyleneimine). Therefore, agglomeration of ZnO particles in thin film was affected the thin film surface roughness and overall morphology. These morphological differences may cause the difference between two fabricated devices. Besides, all devices had same low turn-on voltage (V_{on}). In literature, turn-on voltage is defined as voltage value when luminescence is reached to 1 cd/m^2 [87,88]. Low turn-on voltage indicates low energy consumption and higher operational stability.

Table 3.1 : Comparative characterization for host free Hex-Ir(piq)$_3$ devices.

Device Structure	V_{on}[a] (V)	CE[b] (cd/A)	PE[b] (lm/W)	EQE[b] (%)	L[b] (cd/m^2)	WL_p (nm)
ITO/PEDOT:PSS/Hex-Ir(piq)$_3$/TPBi/Ca/Al	3.5	0.02	0.01	0.02	55.45	623
ITO/BNC/Hex-Ir(piq)$_3$/V_2O_5/Al	3.5	0.04	0.04	0.06	29.66	620
ITO/BNC/Hex-Ir(piq)$_3$/TPD/V_2O_5/Al	3.5	0.60	0.62	0.92	370.60	622
ITO/TNC/Hex-Ir(piq)$_3$/TPD/V_2O_5/Al	3.5	0.50	0.38	0.82	323.70	622

V_{on}, turn-on voltage; CE, current efficiency; PE, power efficiency; EQE, external quantum efficiency; L, luminescence; WL_p, peak wavelength.

[a] The turn on voltage is defined as the applied voltage when luminescence is 1 cd m^{-2}.

[b] The maximum values.

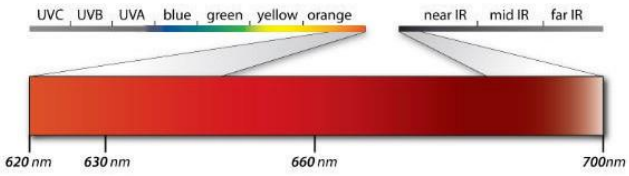

Figure 3.5 : The wavelengths of the red-light.

The wavelengths of the red-light spectrum was shown in Figure 3.5. Peak wavelengths of both conventional (ITO/PEDOT:PSS/Hex-Ir(piq)$_3$/TPBi/Ca/Al) and inverted device (ITO/BNC/Hex-Ir(piq)$_3$/TPD/V_2O_5 /Al) were 623 nm and 622 nm, respectively (Figure 3.6). Hence, both conventional and inverted devices were in the range of red-light. In addition, the sholder seen in the reversible structure at around 670 nm also affected the position of the CIE x,y coordinates. According to the coodinates given in section 3.2, it is seen that the device with inverted structure emited more saturated red light.

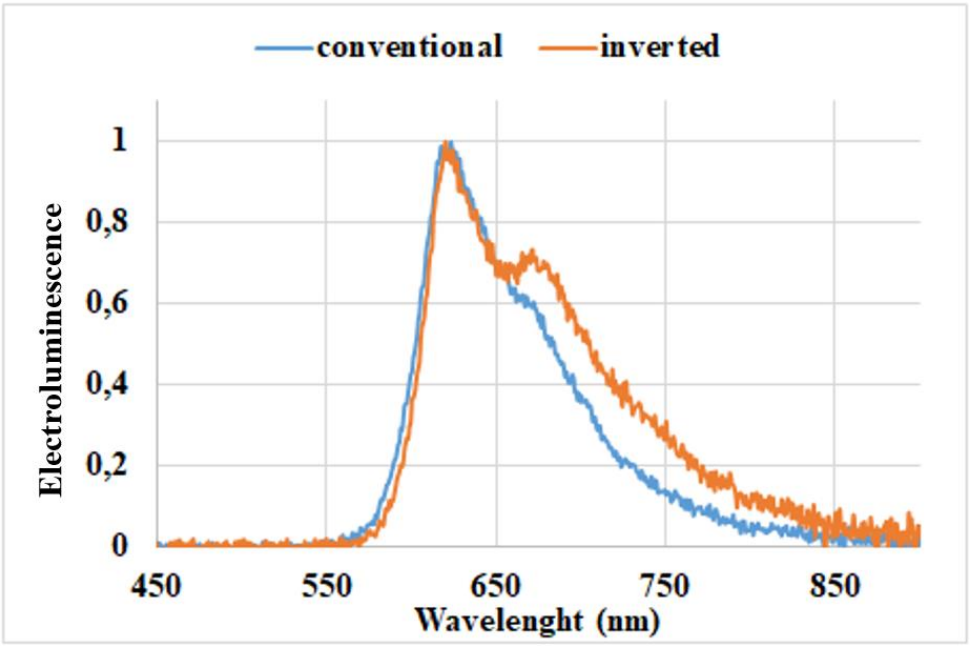

Figure 3.6 : Electroluminescence characteristics of conventional and inverted Hex-Ir(piq)$_3$ without a host devices.

In addition to Hex-Ir(piq)$_3$ without a host study, devices with various different host materials with different doping percentage were fabricated. First of all, using NPD as a host material was experimented. Solutions were prepared with % 5 dopant ratio and 10 mg/ml solution concentration for both conventional and inverted architecture. After spin coating for 50 seconds, all films were cured at 120°C for 10 minutes.

In order to study optimal emissive thin film, different spin coating rates (1000, 1500 and 2000 rpm) were investigated. Conventional device structure was ITO / PEDOT:PSS / Hex-Ir(piq)$_3$: NPD / TPBi / Ca /Al, with this structure all devices were showed great performance with above 1400 cd/m^2 luminescence and 1 cd/A current efficiency. Device fabricated with 2000 rpm spin rate had best performance among other devices as seen in Figure 3.7.

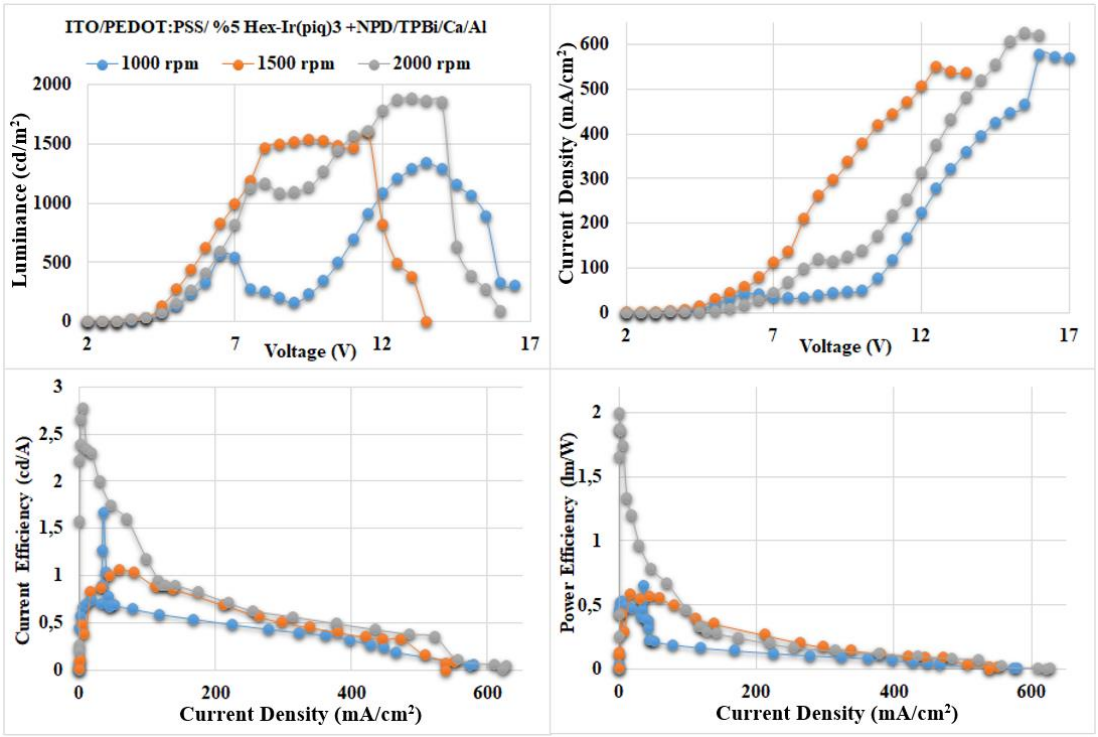

Figure 3.7 : Characterization of conventional Hex-Ir(piq)3 doped NPD devices.

Therefore, for inverted device 2000 rpm was chosen for comparison. There was a drastic performance decrease for inverted device compared to conventional architecture (Figure 3.8). This may be due to hole transport characteristic of NPD, which cause not enough electron transport and less exciton pairing for inverted structure. As seen in Figure 3.9, energy level difference between BNC and EML is great, therefore, another electron injection/transport layer may require for performance improvement of inverted device. But as mentioned before, adding another layer may cause catastrophic thin film deterioration for solution processed devices.

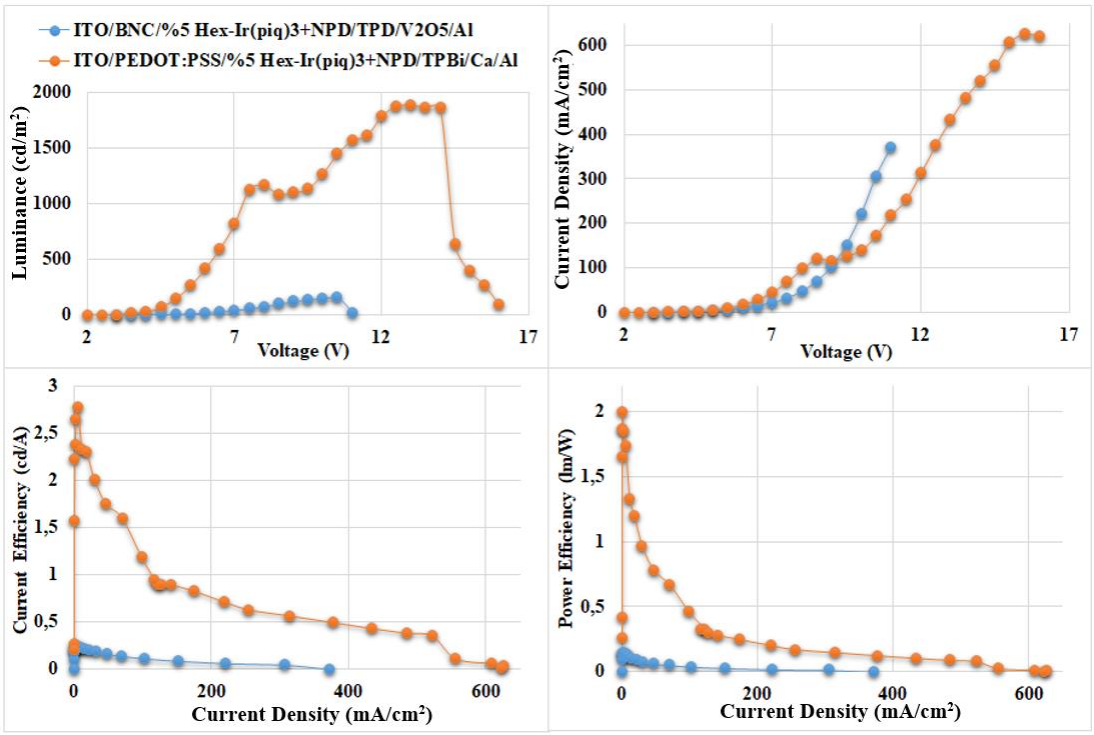

Figure 3.8 : Comparison of conventional and inverted Hex-Ir(piq)3 doped NPD devices.

Peak wavelength was shifted to 617 nm which is reddish orange as seen in Table 3.2. Besides, there was an additional small peak at around 400-450 nm in electroluminescence characteristic of these devices, especially for inverted device it was very distinct (Figure 3.10). This peak was because of contribution from NPD molecule at around 430 nm [89,90]. That shifted emitted color red to pinkish red. Because of performance decrease for inverted devices which restrict AMOLED applications and the color shift effect, it was decided that NPD was not a suitable host for desired outcomes.

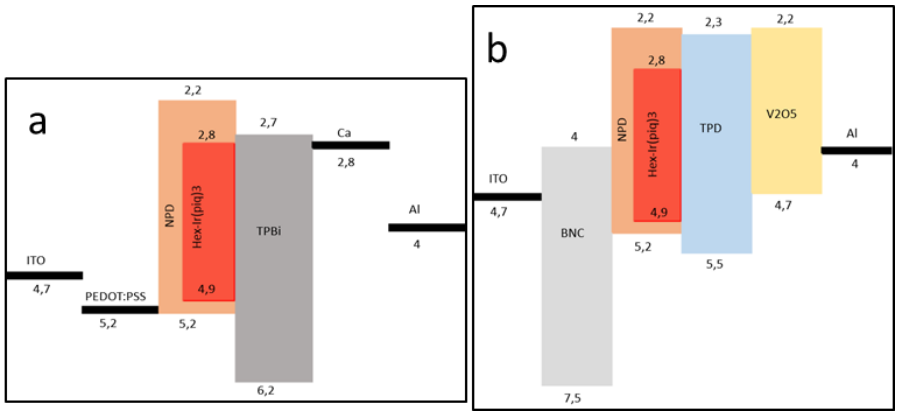

Figure 3.9 : Energy level diagrams of Hex-Ir(piq)$_3$ doped NPD devices a) conventional, b) inverted.

Table 3.2 : Comparative characterization for Hex-Ir(piq)$_3$ doped NPD devices.

Device Structure	V_{on}[a] (V)	CE[b] (cd/A)	PE[b] (lm/W)	EQE[b] (%)	L [b] (cd/m^2)	WL_p (nm)
ITO/PEDOT:PSS/Hex-Ir(piq)$_3$:NPD/TPBi/Ca/Al	3	2.78	1.99	3.14	1889	622
ITO/BNC/Hex-Ir(piq)$_3$:NPD/TPD/V_2O_5/Al	4	0.24	0.15	0.28	157.9	617

V_{on}, turn-on voltage; CE, current efficiency; PE, power efficiency; EQE, external quantum efficiency; L, luminescence; WL_p, peak wavelength.

[a] The turn on voltage is defined as the applied voltage when luminescence is 1 cd m^{-2}.

[b] The maximum values.

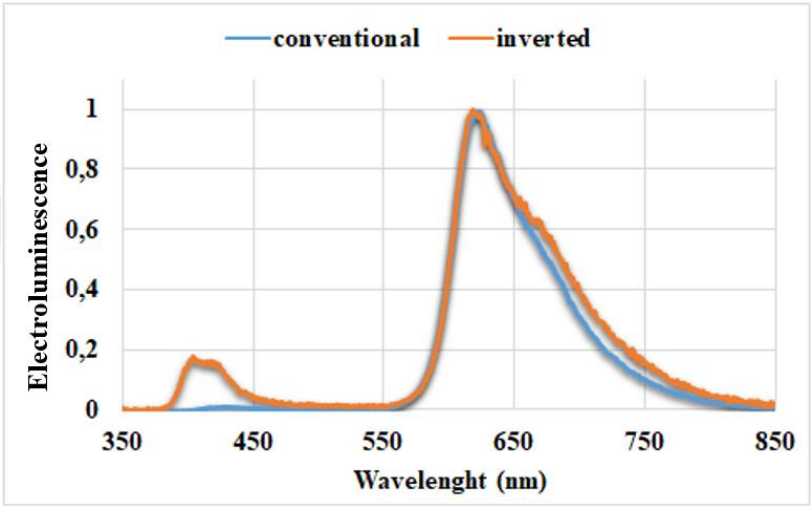

Figure 3.10 : Electroluminescence characteristics of conventional and inverted Hex-Ir(piq)$_3$ doped NPD devices.

Devices were fabricated with many other host materials such as TPBi, CBP and PVK. All devices showed insufficient performance characteristics with less than 1 cd/m^2 luminescence. Lastly, MEH-PPV was chosen for host material because of its red-orange emission color and superior performance with inverted device architecture [2].

In order to determine optimal dopant ratio for Hex-Ir(piq)$_3$ in MEH-PPV for conventional architecture, 15%, 20%, 30% and 40% dopant ratio were investigated for 10 mg/ml solution concentration. Device structure was fabricated as ITO / PEDOT:PSS / Hex-Ir(piq)$_3$: MEH-PPV / Ca /Al. All emissive layer thin films were spin coated at 2500 rpm for 50 seconds and annealed at 120°C for 10 minutes. As seen in Figure 3.11, both luminescence and efficiency values of 20% doped devices were greater than other dopant ratios with almost 300 cd/m^2 luminescence and 0.3 cd/A current efficiency. For further performance improvements, TPBi thin film layer was added as electron transport layer to devices with 15% and 20% dopant ratios.

Fabricated device structure consisted by ITO / PEDOT:PSS / Hex-Ir(piq)$_3$: MEH-PPV / TPBi / Ca /Al. Adding TPBi layer improved electron transport of devices and improved performances of devices as expecting (Figure 3.12). The added TPBi layer made easier the transfer of electrons to the emissive layer. Thus, it facilitated the formation of excitons and luminescence increased from 300 to 1000 cd/m^2. Most importantly, power efficiency increased from 0.1 to 0.25 lm/W for 20% doped devices by adding electron transport layer. 20% dopant ratio showed better performance than 15% as like devices without TPBi. Hence, optimum dopant ratio for conventional architecture was found as 20%.

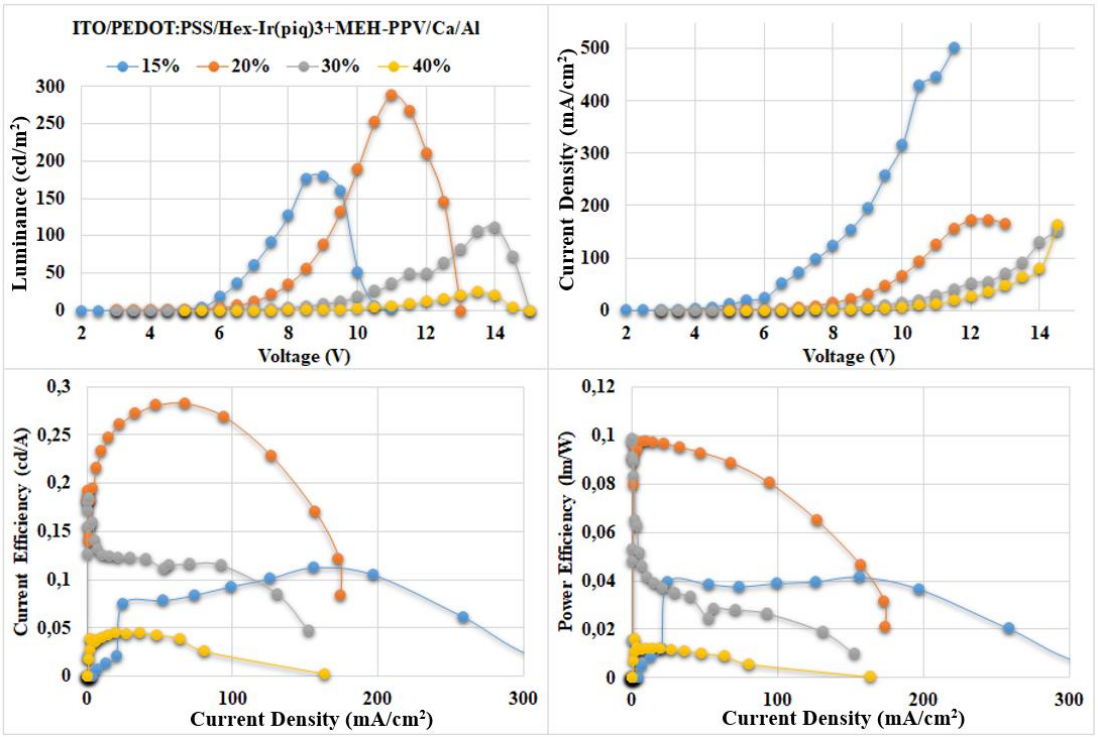

Figure 3.11 : Characterization of conventional Hex-Ir(piq)$_3$ doped MEH-PPV devices without TPBi.

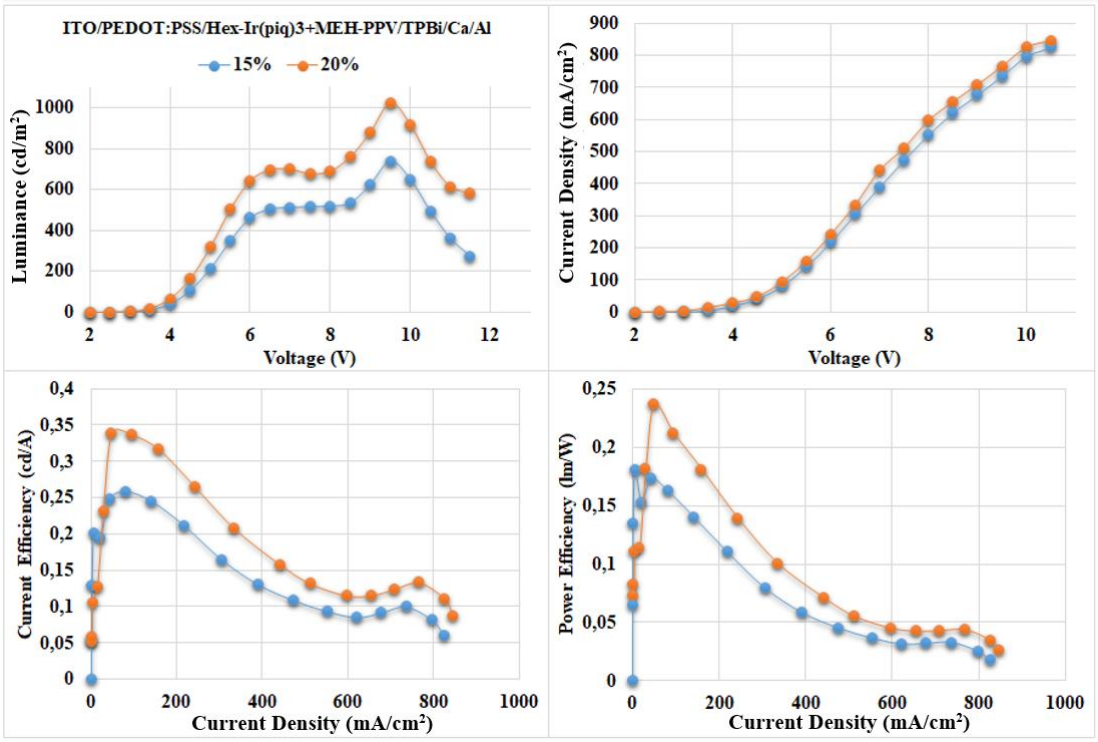

Figure 3.12 : Characterization of conventional Hex-Ir(piq)$_3$ doped MEH-PPV devices with TPBi.

After fabrication and characterization of conventional devices, inverted devices were fabricated with ITO / TNC / Hex-Ir(piq)$_3$: MEH-PPV / V_2O_5 / Al structure and 4 different dopant ratio (10%, 20%, 50% and 80%) were studied. As seen in Figure 3.13, 20% dopant ratio had superior performance among others as like conventional devices. In order to further performance improvement TPD added as hole transport layer the structure and studied. Fabricated device structures were ITO / BNC / Hex-Ir(piq)$_3$: MEH-PPV / TPD /V_2O_5 / Al. In Figure 3.14, 10% and 20% doped devices with TPD and additionally 20% doped device without TPD was shown for comparison. As seen in Table 3.3, overall performances of devices were improved by adding TPD layer. Luminescence value increased from 323 to 1514 cd/m^2, current efficiency was over 2 cd/A and power efficiency was over 1.5 cd/A. Energy level diagram of Hex-Ir(piq)$_3$ doped MEH-PPV devices clarified the performance improvement (Figure 3.15).

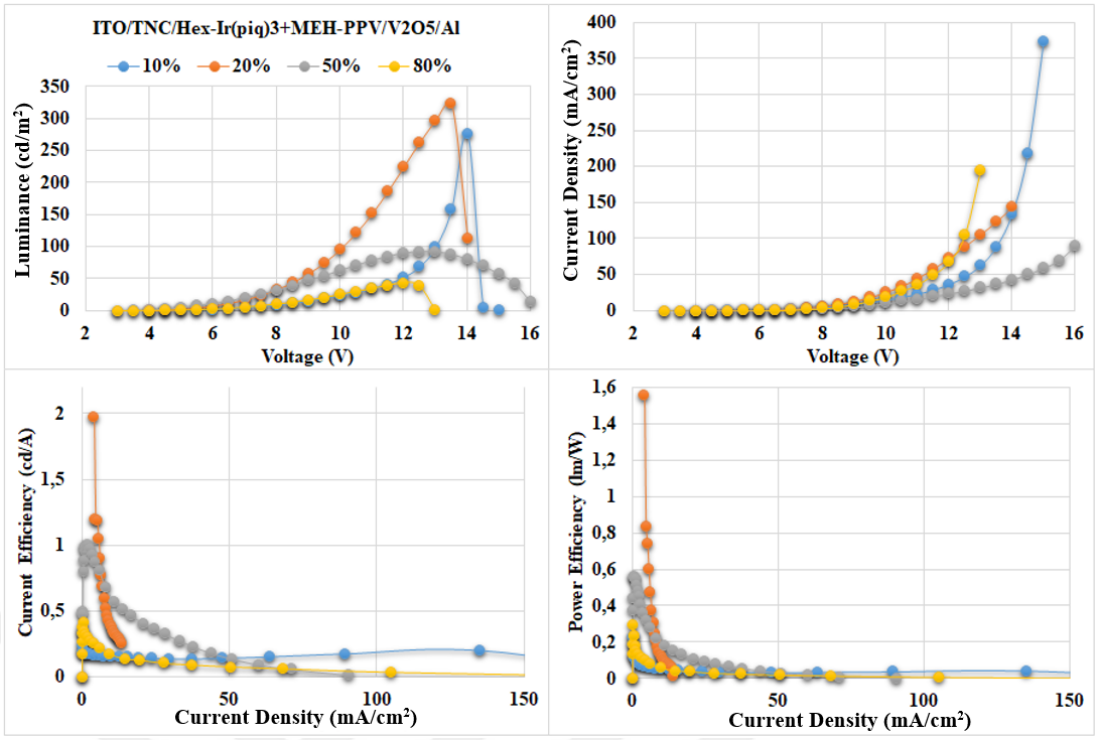

Figure 3.13 : Characterization of inverted Hex-Ir(piq)$_3$ doped MEH-PPV devices without TPD.

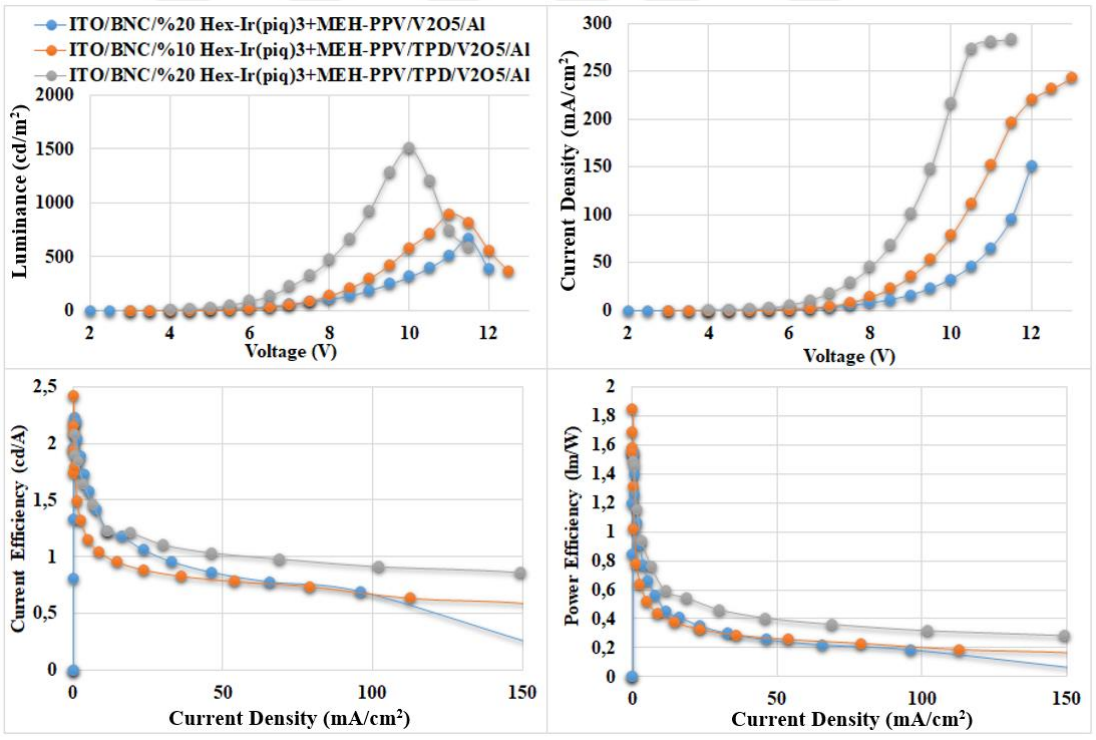

Figure 3.14 : Effect of TPD onto inverted Hex-Ir(piq)$_3$ doped MEH-PPV devices.

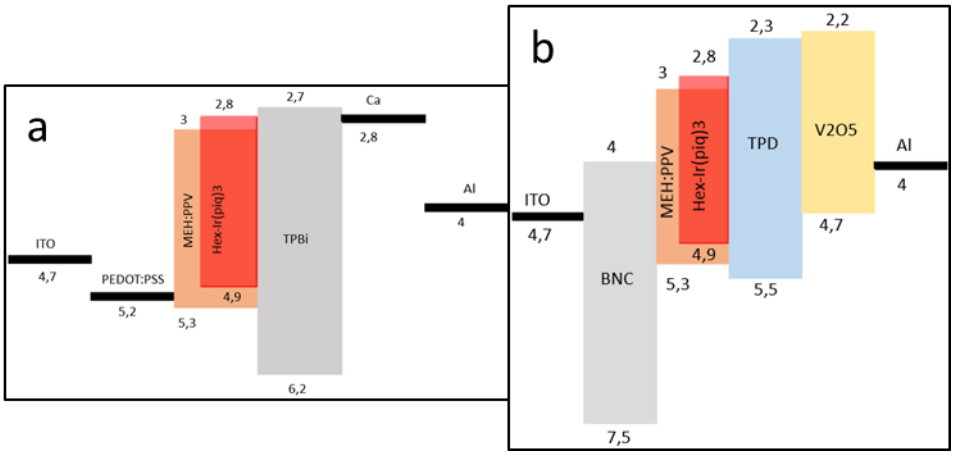

Figure 3.15 : Energy level diagrams of Hex-Ir(piq)$_3$ doped MEH-PPV devices a) conventional, b) inverted.

Table 3.3 : Comparative characterization for Hex-Ir(piq)$_3$ doped MEH-PPV devices.

Device Structure	V_{on}[a] (V)	CE[b] (cd/A)	PE[b] (lm/W)	EQE[b] (%)	L[b] (cd/m^2)	WL_p (nm)
ITO/PEDOT:PSS/Hex-Ir(piq)$_3$:MEH-PPV/Ca/Al	5	0.28	0.09	0.23	289	600
ITO/PEDOT:PSS/Hex-Ir(piq)$_3$:MEH-PPV /TPBi/Ca/Al	3	0.33	0.23	0.22	1025	586
ITO/TNC/Hex-Ir(piq)$_3$:MEH-PPV/V_2O_5/Al	4	1.98	1.56	1.53	323	567
ITO/BNC/Hex-Ir(piq)$_3$:MEH-PPV/V_2O_5/Al	3.5	2.22	1.55	1.62	672	597
ITO/BNC/Hex-Ir(piq)$_3$:MEH-PPV/TPD/V_2O_5 /Al	3.5	2.1	1.5	1.61	1514	597

V_{on}, turn-on voltage; CE, current efficiency; PE, power efficiency; EQE, external quantum efficiency; L, luminescence; WL_p, peak wavelength.

[a] The turn on voltage is defined as the applied voltage when luminescence is 1 cd m^{-2}.

[b] The maximum values.

3.2 CIE Color Coordinates

CIE color coordinates of fabricated devices were shown on CIE chromatically diagram in Figure 3.16. In addition chromaticity coordinates were indicated in Table 3.4. As seen in diagram, Hex-Ir(piq)$_3$ without host devices both conventional and inverted had deepest red color. Adding host material was shifted emitted color to host material original color for both inverted and conventional architecture. As mentioned before, NPD as host shifted deep red color of Hex-Ir(piq)$_3$ molecule to more pinkish red. On the other hand, MEH-PPV as host shifted red color to reddish orange. In addition as seen in diagram MEH-PPV without Hex-Ir(piq)$_3$ guest device was emitted orange and adding Hex-Ir(piq)$_3$ as guest molecule improved the color of

MEH-PPV polymer for applications for RGB OLED system. All fabricated devices of Hex-Ir(piq)$_3$ were in range of red spectrum and could be used as red emitting OLED pixel in RGB display systems.

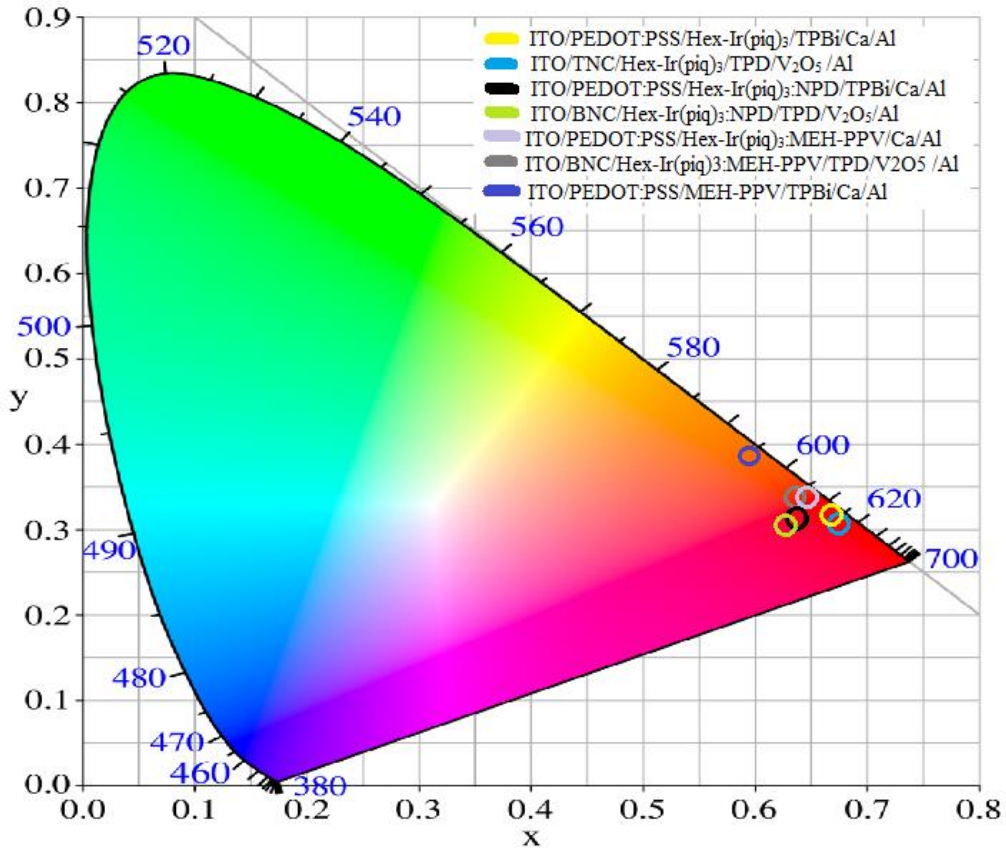

Figure 3.16 : The x,y chromaticity coordinates of fabricated devices, marked in CIE 1931 diagram.

Table 3.4 : x,y chromaticity coordinates of fabricated devices.

Device Structure	Chromatic Coordinates	
	x	y
ITO/PEDOT:PSS/Hex-Ir(piq)$_3$/TPBi/Ca/Al	0.6664	0.333
ITO/TNC/Hex-Ir(piq)$_3$/TPD / V_2O_5/Al	0.6732	0.3211
ITO/PEDOT:PSS/Hex-Ir(piq)$_3$:NPD/TPBi/Ca/Al	0.6343	0.3286
ITO/BNC/Hex-Ir(piq)$_3$:NPD/TPD/V_2O_5 /Al	0.6247	0.3195
ITO/PEDOT:PSS/Hex-Ir(piq)$_3$:MEH-PPV/Ca/Al	0.6446	0.353
ITO/BNC/Hex-Ir(piq)$_3$:MEH-PPV/TPD/V_2O_5 /Al	0.6347	0.3538
ITO/PEDOT:PSS/MEH-PPV/TPBi/Ca/Al	0.5984	0.3999

3.3 Electron Mobility Calculations

As it is known that charge mobility is one of the key parameters for efficiency of OLEDs. Electron mobility is the speed at which electrons move in material in a given direction, in the presence of an electric field. This is important because if electron remains stuck near electrode, there will not be an internal current which leads to emission of light. There are many different methods to calculate electron mobility. Current-voltage characterization, space-charge-limited current method and charge extraction by linearly increasing voltage are some of them [91]. In this study, we used space-charge-limited model (SCLC). SCLC can be described by,

$$J = \frac{9}{8}\varepsilon\varepsilon_0\mu\frac{V^2}{T^3} \quad \textbf{(3.1)}$$

Where J is the current, V is voltage, ε and ε_0 are the relative dielectric constant and the permittivity of the free space, respectively, T is the thickness of the organic layer and μ is the mobility. If J versus V graph is plotted and fitted to $J=AV^2$, the remaining values will be equal to a constant A;

$$A = \frac{9\varepsilon\varepsilon_0\mu}{8T^3} \quad \textbf{(3.2)}$$

From this equation if μ is extracted,

$$\mu = \frac{8AT^3}{9\varepsilon\varepsilon_0} \quad \textbf{(3.3)}$$

The relative dielectric constant ε is assumed to be 3, the permittivity of the free space ε_0 is 8.85×10^{-14} C/Vcm, and thickness of organic layer is 50 nm.

E-only devices were fabricated with MEH-PPV only and 5%, 10%, 20% and 30% Hex-Ir(piq)3 doped MEH-PPV solutions. Electron mobilities of these devices were calculated with explained method above. J versus V graphs were fitted to $J=AV^2$ parabolic equation (Figure 3.17). Then, from A values, μ was calculated. Calculated μ values were shown in Table 3.5. Compared to other doped devices, 20% Hex-$Ir(piq)_3$ doped MEH-PPV thin film was shown highest electron mobility. Likewise, as mentioned in electrical and optical characterization results, 20% doped devices were shown best performance in terms of both luminescence and efficiency. This higher performance can be relevant to higher electron mobility of thin film.

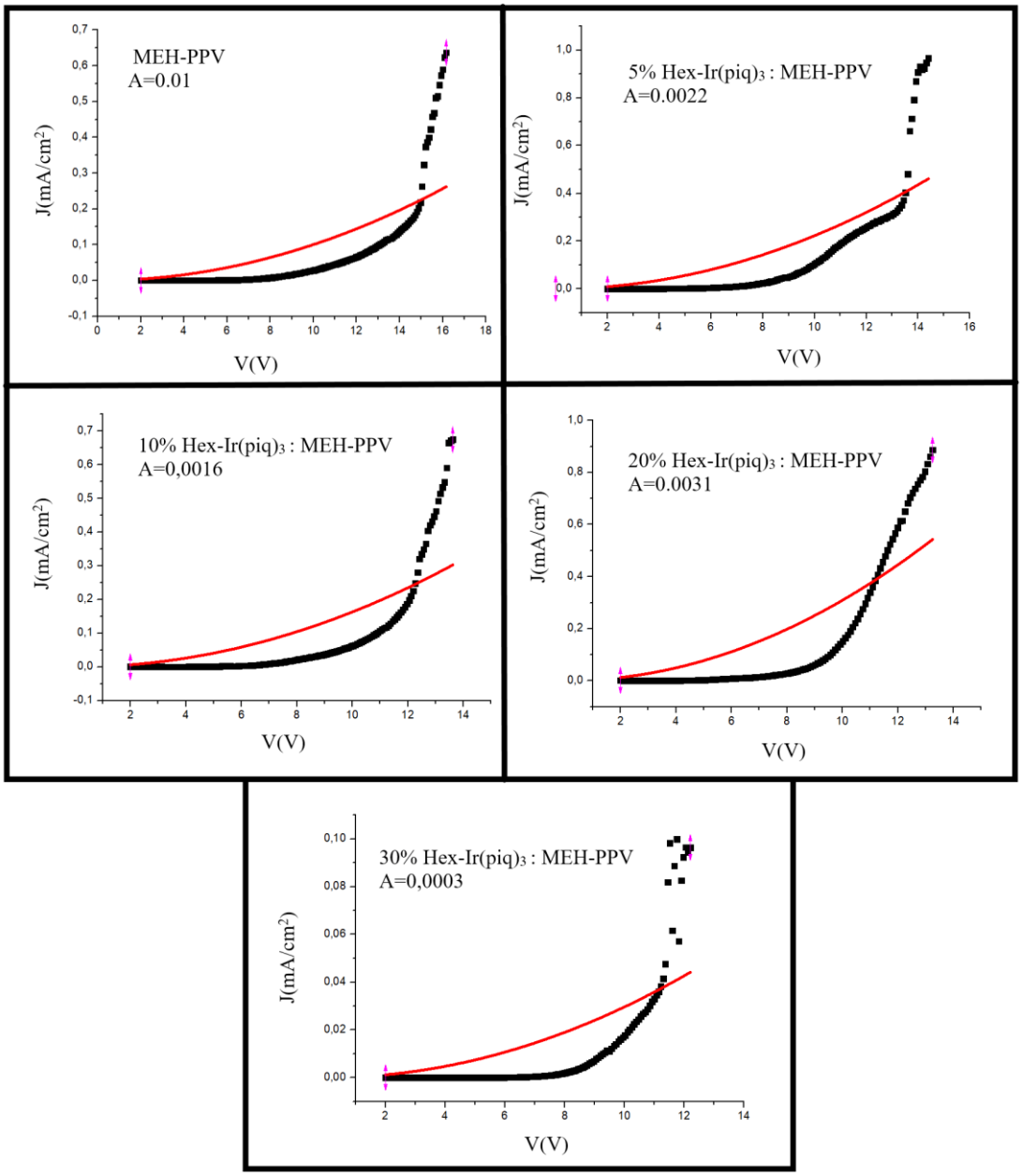

Figure 3.17 : Fitting of J versus V graphs and A values.

Table 3.5 : Electron mobilities of MEH-PPV and Hex-Ir(piq)$_3$ doped MEH-PPV organic layers.

Device Structure	μ ($cm^2V^{-1}s^{-1}$)
Al/MEH-PPV/LiF/Al	4.18×10^{-6}
Al/5% Hex-Ir(piq)$_3$:MEH-PPV/LiF/Al	9.2×10^{-7}
Al/10% Hex-Ir(piq)$_3$:MEH-PPV/LiF/Al	6.82×10^{-7}
Al/20% Hex-Ir(piq)$_3$:MEH-PPV/LiF/Al	1.29×10^{-6}
Al/30% Hex-Ir(piq)$_3$:MEH-PPV/LiF/Al	1.23×10^{-7}

4. CONCLUSION

In this thesis, red OLED fabrication was studied for RGB AMOLED display applications. For this purpose, Hex-Ir(piq)$_3$ molecule was chosen as emissive layer because of its deep red emission color and its potential use for solution processing methods like spin coating or inkjet printing.

Firstly, in order to understand the performance and emissivity of the molecule, host-free device studies have been performed. As a result of these studies, it was observed that the molecule emits red radiation with 622 nm wavelenght. Furthermore, the increase in performance of the molecule with the addition of TPD for the inverted structure shows that hole transfer is critical for this molecule.

Host experiments were firstly performed with fabricating conventional device using the NPD host molecule by refering to the literature. Although this study yielded positive results in the conventional structure, a significant decrease in performance was observed in the inverted structure. In this study, device structure for AMOLED screen was intended and inverted architecture is more applicable for AMOLEDs. It was decided that the NPD host molecule was not suitable for purpose of this study due to the poor performance of the inverted structure and the fact that it was not suitable for AMOLED display systems in terms of emission color.

Experiments were performed with many host molecules that were not included in this study due to low performances. The MEH-PPV polymer was then tested as a host because of its close to red color emission and the known high performance in the inverted structure. As a result of these experiments, more than 1000 cd/m^2 luminescence was obtained in both conventional and inverted structure and more than 2 cd/A current efficiency in inverted structure was obtained for 20% Hex-Ir(piq)$_3$ doped MEH-PPV devices. The electron mobility values measured from fabricated electron only devices are also consistent with the performance values.

When examined in terms of emission color, both NPD and MEH-PPV shifted the emission color slightly. However, all the fabricated devices remained within the red-light spectrum. It is also noteworthy that the addition of Hex-Ir(piq)$_3$ had seriously affected emission color of MEH-PPV.

In conclusion, conventional and inverted OLED devices with enough efficiency were produced which were emitting red color and suitable for use as pixels in AMOLED display applications.

REFERENCES

[1] VanSlyke, S. A., and Tang, C. W. (1985). *U.S. Patent No. 4,539,507*. Washington, DC: U.S. Patent and Trademark Office.

[2] Kaçar, R., Mucur, S. P., Yıldız, F., Dabak, S., and Tekin, E. (2017). Highly efficient inverted organic light emitting diodes by inserting a zinc oxide/polyethyleneimine (ZnO: PEI) nano-composite interfacial layer. *Nanotechnology*, *28*(24), 245204.

[3] Zhao, X. D., Li, Y. Q., Xiang, H. Y., Zhang, Y. B., Chen, J. D., Xu, L. H., and Tang, J. X. (2017). Efficient color-stable inverted white organic light-emitting diodes with outcoupling-enhanced ZnO layer. *ACS applied materials & interfaces*, *9*(3), 2767-2775.

[4] Liu, X., Yao, B., Zhang, Z., Zhao, X., Zhang, B., Wong, W. Y., ... Xie, Z. (2016). Power-efficient solution-processed red organic light-emitting diodes based on an exciplex host and a novel phosphorescent iridium complex. *Journal of Materials Chemistry C*, *4*(24), 5787-5794.

[5] Url-5 < *https://www.research.fsu.edu/research-offices/oc/technologies/metal-halide-perovskite-phosphors-in-leds-for-full-color-display-and-solid-state-lighting* >, date retrieved 04.10.2019.

[6] De Paoli, M. A., and Gazotti, W. A. (2002). Electrochemistry, polymers and opto-electronic devices: a combination with a future. *Journal of the Brazilian Chemical Society*, 13(4), 410-424.

[7] Branas, C., Azcondo, F. J., and Alonso, J. M. (2013). Solid-state lighting: A system review. *IEEE Industrial Electronics Magazine*, *7*(4), 6-14.

[8] Rack, P. D., and Holloway, P. H. (1998). The structure, device physics, and material properties of thin film electroluminescent displays. *Materials Science and Engineering: R: Reports*, *21*(4), 171-219.

[9] Mirov, S., Fedorov, V., Moskalev, I., Martyshkin, D., and Kim, C. (2010). Progress in Cr2+ and Fe2+ doped mid-IR laser materials. *Laser & Photonics Reviews*, *4*(1), 21-41.

[10] Uoyama, H., Goushi, K., Shizu, K., Nomura, H., and Adachi, C. (2012). Highly efficient organic light-emitting diodes from delayed fluorescence. *Nature*, *492*(7428), 234.

[11] Pope, M., Kallmann, H. P., and Magnante, P. J. (1963). Electroluminescence in organic crystals. *The Journal of Chemical Physics*, *38*(8), 2042-2043.

[12] Tang, C. W., and VanSlyke, S. A. (1987). Organic electroluminescent diodes. *Applied physics letters*, *51*(12), 913-915.

[13] Url-13 < *https://electronics.howstuffworks.com/oled3.htm*>, date retrieved 04.10.2019.

[14] Tang, C. W. (1986). Two-layer organic photovoltaic cell. *Applied physics letters*, *48*(2), 183-185.

[15] Träger, F. (Ed.). (2012). *Springer handbook of lasers and optics*. Springer Science & Business Media.

[16] Kepler, R. G., Beeson, P. M., Jacobs, S. J., Anderson, R. A., Sinclair, M. B., Valencia, V. S., and Cahill, P. A. (1995). Electron and hole mobility in tris (8-hydroxyquinolinolato-N1, O8) aluminum. *Applied physics letters*, *66*(26), 3618-3620.

[17] Baldo, M., Deutsch, M., Burrows, P., Gossenberger, H., Gerstenberg, M., Ban, V., and Forrest, S. (1998). Organic vapor phase deposition. *Advanced Materials*, *10*(18), 1505-1514.

[18] Van Slyke, S. A., Chen, C. H., and Tang, C. W. (1996). Organic electroluminescent devices with improved stability. *Applied physics letters*, *69*(15), 2160-2162.

[19] Shirota, Y., Kuwabara, Y., Inada, H., Wakimoto, T., Nakada, H., Yonemoto, Y., ... and Imai, K. (1994). Multilayered organic electroluminescent device using a novel starburst molecule, 4, 4', 4 '-tris (3-methylphenylphenylamino) triphenylamine, as a hole transport material. *Applied Physics Letters*, *65*(7), 807-809.

[20] Yamamori, A., Adachi, C., Koyama, T., and Taniguchi, Y. (1998). Doped organic light emitting diodes having a 650-nm-thick hole transport layer. *Applied Physics Letters*, *72*(17), 2147-2149.

[21] Blochwitz, J., Pfeiffer, M., Fritz, T., and Leo, K. (1998). Low voltage organic light emitting diodes featuring doped phthalocyanine as hole transport material. *Applied Physics Letters*, *73*(6), 729-731.

[22] Chiba, T., Pu, Y. J., and Kido, J. (2015). Solution-processable electron injection materials for organic light-emitting devices. *Journal of Materials Chemistry C*, *3*(44), 11567-11576.

[23] Sessolo, M., and Bolink, H. J. (2011). Hybrid organic–inorganic light-emitting diodes. *Advanced Materials*, *23*(16), 1829-1845.

[24] Tokmoldin, N., Griffiths, N., Bradley, D. D., and Haque, S. A. (2009). A Hybrid Inorganic–Organic Semiconductor Light-Emitting Diode Using ZrO2 as an Electron-Injection Layer. *Advanced Materials*, *21*(34), 3475-3478.

[25] Meyer, J., Hamwi, S., Kröger, M., Kowalsky, W., Riedl, T., and Kahn, A. (2012). Transition metal oxides for organic electronics: energetics, device physics and applications. *Advanced Materials*, *24*(40), 5408-5427.

[26] Fukagawa, H., Morii, K., Hasegawa, M., Arimoto, Y., Kamada, T., Shimizu, T., and Yamamoto, T. (2014). Highly efficient and air-stable inverted organic light-emitting diode composed of inert materials. *Applied Physics Express*, *7*(8), 082104.

[27] De Bruyn, P., Moet, D. J. D., and Blom, P. W. M. (2012). All-solution processed polymer light-emitting diodes with air stable metal-oxide electrodes. *Organic Electronics*, *13*(6), 1023-1030**.**

[28] Deng, Z. B., Ding, X. M., Lee, S. T., and Gambling, W. A. (1999). Enhanced brightness and efficiency in organic electroluminescent devices using SiO 2 buffer layers. *Applied Physics Letters*, *74*(15), 2227-2229.

[29] Romero, D. B., Schaer, M., Zuppiroli, L., Cesar, B., and Francois, B. (1995). Effects of doping in polymer light-emitting diodes. *Applied physics letters*, *67*(12), 1659-1661.

[30] Huang, F., MacDiarmid, A. G., and Hsieh, B. R. (1997). An iodine-doped polymer light-emitting diode. *Applied physics letters*, *71*(17), 2415-2417.

[31] Blochwitz, J., Pfeiffer, M., Fritz, T., and Leo, K. (1998). Low voltage organic light emitting diodes featuring doped phthalocyanine as hole transport material. *Applied Physics Letters*, *73*(6), 729-731.

[32] Elschner, A., Bruder, F., Heuer, H. W., Jonas, F., Karbach, A., Kirchmeyer, S., ... and Wehrmann, R. (2000). PEDT/PSS for efficient hole-injection in hybrid organic light-emitting diodes. *Synthetic metals*, *111*, 139-143

[33] Nguyen, T. P., Le Rendu, P., Long, P. D., and De Vos, S. A. (2004). Chemical and thermal treatment of PEDOT: PSS thin films for use in organic light emitting diodes. *Surface and Coatings Technology*, *180*, 646-649.

[34] De Kok, M. M., Buechel, M., Vulto, S. I. E., Van de Weijer, P., Meulenkamp, E. A., De Winter, S. H. P. M., ... and Van Elsbergen, V. (2004). Modification of PEDOT: PSS as hole injection layer in polymer LEDs. *physica status solidi (a)*, *201*(6), 1342-1359.

[35] Brown, T. M., Kim, J. S., Friend, R. H., Cacialli, F., Daik, R., and Feast, W. J. (1999). Built-in field electroabsorption spectroscopy of polymer light-emitting diodes incorporating a doped poly (3, 4-ethylene dioxythiophene) hole injection layer. *Applied Physics Letters*, *75*(12), 1679-1681.

[36] Adachi, C., Tsutsui, T., and Saito, S. (1989). Organic electroluminescent device having a hole conductor as an emitting layer. *Applied Physics Letters*, *55*(15), 1489-1491.

[37] Kido, J., Nagai, K., and Okamoto, Y. (1993). Bright organic electroluminescent devices with double-layer cathode. *IEEE Transactions on Electron Devices*, *40*(7), 1342-1344.

[38] Desai, P., Shakya, P., Kreouzis, T., Gillin, W. P., Morley, N. A., and Gibbs, M. R. J. (2007). Magnetoresistance and efficiency measurements of Al q 3-based OLEDs. *Physical Review B*, *75*(9), 094423.

[39] Li, C. N., Kwong, C. Y., Djurišić, A. B., Lai, P. T., Chui, P. C., Chan, W. K., and Liu, S. Y. (2005). Improved performance of OLEDs with ITO surface treatments. *Thin Solid Films*, *477*(1-2), 57-62.

[40] Halls, M. D., Tripp, C. P., and Schlegel, H. B. (2001). Structure and infrared (IR) assignments for the OLED material: N, N′-diphenyl-N, N′-bis (1-naphthyl)-1, 1′-biphenyl-4, 4 ″-diamine (NPB). *Physical Chemistry Chemical Physics*, *3*(11), 2131-2136**.**

[41] Choong, V. E., Shi, S., Curless, J., Shieh, C. L., Lee, H. C., So, F., ... and Yang, J. (1999). Organic light-emitting diodes with a bipolar transport layer. *Applied Physics Letters*, *75*(2), 172-174.

[42] Zheng, Y., Eom, S. H., Chopra, N., Lee, J., So, F., and Xue, J. (2008). Efficient deep-blue phosphorescent organic light-emitting device with improved electron and exciton confinement. *Applied Physics Letters*, *92*(22), 196.

[43] Yeh, S. J., Wu, M. F., Chen, C. T., Song, Y. H., Chi, Y., Ho, M. H., ... and Chen, C. H. (2005). New dopant and host materials for blue-light-emitting phosphorescent organic electroluminescent devices. *Advanced Materials*, *17*(3), 285-289.

[44] Yeh, S. J., Wu, M. F., Chen, C. T., Song, Y. H., Chi, Y., Ho, M. H., ... and Chen, C. H. (2005). New dopant and host materials for blue-light-emitting phosphorescent organic electroluminescent devices. *Advanced Materials*, *17*(3), 285-289.

[45] Vecchi, P. A., Padmaperuma, A. B., Qiao, H., Sapochak, L. S., and Burrows, P. E. (2006). A dibenzofuran-based host material for blue electrophosphorescence. *Organic letters*, *8*(19), 4211-4214.

[46] Tsai, M. H., Lin, H. W., Su, H. C., Ke, T. H., Wu, C. C., Fang, F. C., ... and Wu, C. I. (2006). Highly efficient organic blue electrophosphorescent devices based on 3, 6-bis (triphenylsilyl) carbazole as the host material. *Advanced Materials*, *18*(9), 1216-1220.

[47] Gebeyehu, D., Walzer, K., He, G., Pfeiffer, M., Leo, K., Brandt, J., ... and Vestweber, H. (2005). Highly efficient deep-blue organic light-emitting diodes with doped transport layers. *Synthetic metals*, *148*(2), 205-211.

[48] Yang, Q., Hao, Y., Wang, Z., Li, Y., Wang, H., and Xu, B. (2012). Double-emission-layer green phosphorescent OLED based on LiF-doped TPBi as electron transport layer for improving efficiency and operational lifetime. *Synthetic Metals*, *162*(3-4), 398-401.

[49] Partridge, R. H. (1976). *U.S. Patent No. 3,995,299*. Washington, DC: U.S. Patent and Trademark Office.

[50] Partridge, R. H. (1983). Electroluminescence from polyvinylcarbazole films: 1. Carbazole cations. *Polymer*, *24*(6), 733-738.

[51] Burroughes, J. H., Bradley, D. D., Brown, A. R., Marks, R. N., Mackay, K., Friend, R. H., ... and Holmes, A. B. (1990). Light-emitting diodes based on conjugated polymers. *nature*, *347*(6293), 539.

[52] Baigent, D. R., Greenham, N. C., Grüner, J., Marks, R. N., Friend, R. H., Moratti, S. C., & Holmes, A. B. (1994). Light-emitting diodes fabricated with conjugated polymers—recent progress. *Synthetic Metals*, *67*(1-3), 3-10.

[53] Segura, J. L. (1998). The chemistry of electroluminescent organic materials. *Acta polymerica*, *49*(7), 319-344.

[54] Friend, R. H., Gymer, R. W., Holmes, A. B., Burroughes, J. H., Marks, R. N., Taliani, C. D. D. C., ... and Salaneck, W. R. (1999). Electroluminescence in conjugated polymers. *nature*, *397*(6715), 121.

[55] Mitschke, U., and Bäuerle, P. (2000). The electroluminescence of organic materials. *Journal of Materials Chemistry*, *10*(7), 1471-1507.

[56] Rees, I. D., Robinson, K. L., Holmes, A. B., Towns, C. R., and O'Dell, R. (2002). Recent developments in light-emitting polymers. *MRS bulletin*, *27*(6), 451-455.

[57] Babudri, F., Farinola, G. M., and Naso, F. (2004). Synthesis of conjugated oligomers and polymers: the organometallic way. *Journal of Materials Chemistry*, *14*(1), 11-34.

[58] Akcelrud, L. (2003). Electroluminescent polymers. *Progress in Polymer Science*, *28*(6), 875-962.

[59] Rault-Berthelot, J., Granger, M. M., and Mattiello, L. (1998). Anodic oxidation of 9, 9′-spirobifluorene in CH2Cl2+ 0.2 M Bu4NBF4. Electrochemical behaviour of the derived oxidation product. *Synthetic metals*, *97*(3), 211-215.

[60] Bernius, M. T., Inbasekaran, M., O'Brien, J., and Wu, W. (2000). Progress with light-emitting polymers. *Advanced Materials*, *12*(23), 1737-1750.

[61] Bernius, M., Inbasekaran, M., Woo, E., Wu, W., and Wujkowski, L. (2000). Fluorene-based polymers-preparation and applications. *Journal of Materials Science: Materials in Electronics*, *11*(2), 111-116.

[62] Leclerc, M. (2001). Polyfluorenes: twenty years of progress. *Journal of Polymer Science Part A: Polymer Chemistry*, *39*(17), 2867-2873.

[63] Neher, D. (2001). Polyfluorene homopolymers: conjugated liquid-crystalline polymers for bright blue emission and polarized electroluminescence. *Macromolecular Rapid Communications*, *22*(17), 1365-1385.

[64] Scherf, U., and List, E. J. (2002). Semiconducting polyfluorenes—towards reliable structure–property relationships. *Advanced Materials*, *14*(7), 477-487.

[65] Wu, W., Inbasekaran, M., Hudack, M., Welsh, D., Yu, W., Cheng, Y., ... and Fletcher, R. (2004). Recent development of polyfluorene-based RGB materials for light emitting diodes. *Microelectronics journal*, *35*(4), 343-348.

[66] Baldo, M., Lamansky, S., Burrows, P., Thompson, M., and Forrest, S. (1999). Very high-efficiency green organic light-emitting devices based on electrophosphorescence. *Applied Physics Letters*, *75*(1), 4-6.

[67] Cui, J., Wang, A., Edleman, N. L., Ni, J., Lee, P., Armstrong, N. R., and Marks, T. J. (2001). Indium Tin Oxide Alternatives—High Work Function Transparent Conducting Oxides as Anodes for Organic Light-Emitting Diodes. *Advanced materials*, *13*(19), 1476-1480.

[68] Chen, Y., Yue, Y. Y., Wang, S. R., Zhang, N., Feng, J., and Sun, H. B. (2019). Graphene as a Transparent and Conductive Electrode for Organic Optoelectronic Devices. *Advanced Electronic Materials*, 1900247.

[69] Han, T. H., Lee, Y., Choi, M. R., Woo, S. H., Bae, S. H., Hong, B. H., ... and Lee, T. W. (2012). Extremely efficient flexible organic light-emitting diodes with modified graphene anode. *Nature Photonics*, *6*(2), 105.

[70] Wu, J., Agrawal, M., Becerril, H. A., Bao, Z., Liu, Z., Chen, Y., and Peumans, P. (2009). Organic light-emitting diodes on solution-processed graphene transparent electrodes. *ACS nano*, *4*(1), 43-48.

[71] Tang, C. W., VanSlyke, S. A., and Chen, C. H. (1989). Electroluminescence of doped organic thin films. *Journal of Applied Physics*, *65*(9), 3610-3616.

[72] Hung, L. S., Tang, C. W., and Mason, M. G. (1997). Enhanced electron injection in organic electroluminescence devices using an Al/LiF electrode. *Applied Physics Letters*, *70*(2), 152-154.

[73] Shaheen, S. E., Jabbour, G. E., Morrell, M. M., Kawabe, Y., Kippelen, B., Peyghambarian, N., ... and Armstrong, N. R. (1998). Bright blue organic light-emitting diode with improved color purity using a LiF/Al cathode. *Journal of applied physics*, *84*(4), 2324-2327.

[74] Jabbour, G. E., Wang, J. F., Kippelen, B., and Peyghambarian, N. (1999). Sharp red organic light-emitting devices with enhanced efficiency. *Japanese journal of applied physics*, *38*(12B), L1553.

[75] Staudigel, J., Stößel, M., Steuber, F., and Simmerer, J. (1999). A quantitative numerical model of multilayer vapor-deposited organic light emitting diodes. *Journal of Applied Physics*, *86*(7), 3895-3910.

[76] Li, Q., Li, J., Ren, H., Duan, Y., Gao, Z., and Liu, D. (2011). Solution-processible Thieno-[3, 4-b]-pyrazine Derivatives with Large Stokes Shifts for Non-doped Red Light-emitting Diodes. *Macromolecular rapid communications*, *32*(9-10), 736-743.

[77] Lunt, R. R., Benziger, J. B., and Forrest, S. R. (2010). Relationship between crystalline order and exciton diffusion length in molecular organic semiconductors. *Advanced Materials*, *22*(11), 1233-1236.

[78] Hofmann, S., Rosenow, T. C., Gather, M. C., Lüssem, B., and Leo, K. (2012). Singlet exciton diffusion length in organic light-emitting diodes. *Physical Review B*, *85*(24), 245209.

[79] Lewis, A. J., Ruseckas, A., Gaudin, O. P. M., Webster, G. R., Burn, P. L., and Samuel, I. D. W. (2006). Singlet exciton diffusion in MEH-PPV films studied by exciton–exciton annihilation. *Organic Electronics*, *7*(6), 452-456.

[80] Lunt, R. R., Giebink, N. C., Belak, A. A., Benziger, J. B., and Forrest, S. R. (2009). Exciton diffusion lengths of organic semiconductor thin films measured by spectrally resolved photoluminescence quenching. *Journal of Applied Physics*, *105*(5), 053711.

[81] Shi, J., and Tang, C. W. (1997). Doped organic electroluminescent devices with improved stability. *Applied physics letters*, *70*(13), 1665-1667.

[82] Baldo, M. A., Thompson, M. E., and Forrest, S. R. (2000). High-efficiency fluorescent organic light-emitting devices using a phosphorescent sensitizer. *Nature*, *403*(6771), 750.

[83] Chao, Y. C., Huang, S. Y., Chen, C. Y., Chang, Y. F., Meng, H. F., Yen, F. W., ... and Horng, S. F. (2011). Highly efficient solution-processed red organic light-emitting diodes with long-side-chained triplet emitter. *Synthetic Metals*, *161*(1-2), 148-152.

[84] Kim, J., Song, J., Park, S., and Yu, J. W. (2017). Buffer layer control for solution processing of white organic light-emitting diodes. *Macromolecular Research*, *25*(9), 944-949.

[85] Park, S., Lim, S. J., Kim, J., and Yu, J. W. (2017). Organic light-emitting diodes with an internal light extraction layer prepared by intense pulsed light. *Macromolecular Research*, *25*(10), 1022-1027.

[86] Kaçar, R., Mucur, S. P., Yıldız, F., Dabak, S., and Tekin, E. (2018). Solution processed ternary blend nano-composite charge regulation layer to enhance inverted OLED performances. *Applied Physics Letters*, *112*(16), 163302.

[87] Yu, J., Wang, J., Lou, S., Wang, T., and Jiang, Y. (2008). Small molecular and polymer organic light-emitting diodes based on novel iridium complex phosphor. *Displays*, *29*(5), 493-496.

[88] Yap, C. C., Yahaya, M., and Salleh, M. M. (2008). Influence of thickness of functional layer on performance of organic salt-doped OLED with ITO/PVK: PBD: TBAPF6/Al structure. *Current Applied Physics*, *8*(5), 637-644.

[89] Sun, Y., Giebink, N. C., Kanno, H., Ma, B., Thompson, M. E., and Forrest, S. R. (2006). Management of singlet and triplet excitons for efficient white organic light-emitting devices. *Nature*, *440*(7086), 908.

[90] D'Andrade, B. W., Brooks, J., Adamovich, V., Thompson, M. E., and Forrest, S. R. (2002). White light emission using triplet excimers in electrophosphorescent organic light-emitting devices. *Advanced Materials*, *14*(15), 1032-1036.

[91] Amorim, C. A., Cavallari, M. R., Santos, G., Fonseca, F. J., Andrade, A. M., and Mergulhão, S. (2012). Determination of carrier mobility in MEH-PPV thin-films by stationary and transient current techniques. *Journal of Non-Crystalline Solids*, *358*(3), 484-491.

CURRICULUM VITAE

Name Surname **: Ahu Galen ALTAŞ**

Place and Date of Birth **: İstanbul, 21.08.1993**

E-Mail **: galenaltas@gmail.com**

EDUCATION **:**

- **B.Sc.** **:** 2016, Yıldız Technical University, Faculty of Chemical and Metallurgical Engineering,Chemical Engineering

PROFESSIONAL EXPERIENCE AND REWARDS:

Projects:

- 320 x 240 Pixel RGB AMOLED Avionics Display Development Project, TUBITAK, 1007 program, Project Scholar, Project no: 113G035.
- National Development of Ultra-thin Glasses and Technology Demonstration Prototype Production for Display Technologies, TUBITAK, 1003 program, Project Scholar, Project no: 117E708.